

# Integrated Approaches Revealed the Therapeutic Mechanisms of Zuojin Pill Against Gastric Mucosa Injury in a Rat Model with Chronic Atrophic Gastritis

Lisheng Chen<sup>1,2</sup>, Tingting He<sup>3</sup>, Ruilin Wang<sup>3</sup>, Honghong Liu<sup>4</sup>, Xin Wang<sup>1,2</sup>, Haotian Li<sup>2</sup>, Manyi Jing<sup>2</sup>, Xuelin Zhou<sup>5</sup>, Shizhang Wei<sup>6</sup>, Wenjun Zou<sup>1</sup>, Yanling Zhao<sup>1,2</sup>

<sup>1</sup>College of Pharmacy, Chengdu University of Traditional Chinese Medicine, Chengdu, People's Republic of China; <sup>2</sup>Department of Pharmacy Department, The Fifth Medical Center of Chinese PLA General Hospital, Beijing, People's Republic of China; <sup>3</sup>Division of Integrative Medicine, The Fifth Medical Center of General Hospital of PLA, Beijing, People's Republic of China; <sup>4</sup>Integrated TCM & Western Medicine Department, The Fifth Medical Center of Chinese PLA General Hospital, Beijing, People's Republic of China; <sup>5</sup>Department of Pharmacology, School of Basic Medical Sciences, Capital Medical University, Beijing, People's Republic of China; <sup>6</sup>Department of Anatomy, Histology and Embryology, School of Basic Medical Sciences, Peking University, Beijing, People's Republic of China

Correspondence: Yanling Zhao, Department of Pharmacy, The Fifth Medical Center of Chinese PLA General Hospital, Beijing, People's Republic of China, Email zhaoyl2855@126.com; Wenjun Zou, College of Pharmacy, Chengdu University of Traditional Chinese Medicine, Chengdu, People's Republic of China, Email zouwenjun@163.com

**Background:** The Zuojin Pill (ZJP) is widely used for treating chronic atrophic gastritis (CAG) in clinical practice, effectively ameliorating symptoms such as vomiting, pain, and abdominal distension in patients. However, the underlying mechanisms of ZJP in treating CAG has not been fully elucidated.

**Purpose:** This study aimed to clarify the characteristic function of ZJP in the treatment of CAG and its potential mechanism.

**Methods:** The CAG model was established by alternant administrations of ammonia solution and sodium deoxycholate, as well as an irregular diet. Therapeutic effects of ZJP on body weight, serum biochemical indexes and general condition were analyzed. HE staining and AB-PAS staining were analyzed to characterize the mucosal injury and the thickness of gastric mucosa. Furthermore, network pharmacology and molecular docking were used to predict the regulatory mechanism and main active components of ZJP in CAG treatment. RT-PCR, immunohistochemistry, immunofluorescence and Western blotting were used to measure the expression levels of apoptosis-related proteins, gastric mucosal barrier-associated proteins and PI3K/Akt signaling pathway proteins.

**Results:** The results demonstrated that ZJP significantly improved the general state of CAG rats, alleviated weight loss and gastric histological damage and reduced the serum biochemical indicators. Network pharmacology and molecular docking found that ZJP in treating CAG by inhibiting inflammation, suppressing apoptosis, and protecting the gastric mucosal barrier via the PI3K/Akt signaling pathway. Further experiments confirmed that ZJP obviously modulated the expression of key proteins involved in gastric mucosal cell apoptosis, such as Bax, Bad, Apaf-1, cleaved-caspase-3, cleaved-caspase-9, Cytochrome C, Bcl-2, and Bcl-xl. Moreover, ZJP significantly reversed the protein expression of Occludin, ZO-1, Claudin-4 and E-cadherin.

**Conclusion:** Our study revealed that ZJP treats CAG by inhibiting the PI3K/Akt signaling pathway. This research provided a scientific basis for the rational use of ZJP in clinical practice.

**Keywords:** Zuojin Pill, chronic atrophic gastritis, network pharmacology, molecular docking, PI3K/Akt signaling pathway

## Introduction

Chronic atrophic gastritis (CAG) is a gastric disease with pathological characteristics of reduced gastric acid secretion, atrophic gastric mucosa and metaplasia of intestine epithelium.<sup>1,2</sup> CAG is considered a key precancerous lesion in gastric cancer, which is the third leading cause of cancer death reported in the global cancer statistics for 2018.<sup>3</sup> Previous studies have shown that CAG is caused by a combination of factors, including helicobacter pylori infection, inadequate immune

regulation and impaired energy metabolism, and that its pathogenesis is related to oxidative stress, inflammation, endothelial and mucosal dysfunction.<sup>4,5</sup> The current clinical treatment of CAG relies mainly on the agents used for gastric mucosal protection and symptom relief, vitamin C supplementation and proton pump inhibitors, which limit their clinical application due to their long course, aggressiveness and side effects.<sup>6,7</sup> Therefore, there is an urgent need for complementary and alternative treatments for CAG.

Traditional Chinese medicine (TCM) has unique advantages in the treatment of CAG due to its dual therapeutic and coordinating functions, wide range of applications and few side effects.<sup>8–11</sup> The classic Chinese prescription Zuojin Pill (ZJP) is recorded in “Danxi prescription therapy” in the Yuan Dynasty. It is a famous TCM formula in clinic used for the treatment of CAG, which consists of two herbs including *Coptidis Rhizoma* and *Euodiae Fructus*.<sup>12</sup> Modern pharmacological researches have shown that ZJP has various effects such as anti-inflammation,<sup>12</sup> antibacterial,<sup>13</sup> anti-apoptosis<sup>14</sup> and mucosal protection,<sup>15</sup> which exhibits remarkable therapeutic effects on digestive disorders. A recent study found that ZJP acts as an inflammatory inhibitor to regulate comprehensive metabolic disorders in clinic, which is an important mechanism of ZJP in the treatment of chronic gastritis.<sup>16</sup> However, the mechanism of ZJP for the treatment of chronic atrophic gastritis is not fully understood. Therefore, an exploration into the underlying mechanism of ZJP in the treatment of CAG is necessary.

With the rapid development of bioinformatics, an emerging network pharmacology has been proposed which uses mathematical and computable representations to represent the various links between herbal formulations and diseases.<sup>17</sup> Network pharmacology provides a new idea for drug research, especially for TCM research based on complex system. Accumulating evidence shows that network pharmacology can elucidate the potential mechanisms of action of multi-component, multi-target drugs through the analysis of various complex, multi-level interaction networks.<sup>18,19</sup> Molecular docking technology is a common tool used to explore the interaction sites between small molecules and macromolecules. The study aims to elucidate the characteristic effects of ZJP on the histopathological improvement of gastric tissue in CAG by integrating experimental methods, providing experimental evidence for the clinical rational application of ZJP in treating CAG; Through high-throughput analysis methods such as network pharmacology and molecular docking, it aims to reveal the molecular biological mechanisms of ZJP in treating CAG and potential active substances, providing data support for future development of new drugs based on ZJP for treating CAG (Figure 1).

## Materials and Methods

### Reagents

*Coptidis Rhizoma* (Lot: 21030801) and *Euodiae Fructus* (Lot: 21101401) were purchased from Beijing LVYE Pharmaceutical Co., Ltd. (Beijing, China). Sodium deoxycholate (Lot: CD33141310) and ammonia (Lot: 2023AS0328) were provided by Beijing Zhongke Ruijin Technology Co., Ltd. and Biotechnology Co., Ltd., respectively. Vitacoenzyme tablets (Lot No. 221002) were obtained from Guangxi Dahai Sunshine Pharmaceutical Co., Ltd. All antibodies and the related reagents were obtained from commercial sources.

### Preparation of ZJP

*Coptidis Rhizoma* and *Euodiae Fructus* (6:1, w/w) were soaked in pure water for 30 min. Then, it was extracted twice by heating (1h at a time). After that, all filtrates were rotary evaporated, concentrated, dried into dry powder and stored at 4 °C.<sup>20</sup> The weight ratio of ZJP was 18.75%.

### Animals and Experimental Design

Specific pathogen free (SPF) male Sprague-Dawley rats (180–200g) were obtained from Sibeifu Biotechnology Co., Ltd. (Beijing, China, license No.: SCXK (Beijing) 2019–0010). All the rats were kept in ventilated polypropylene cages at room temperature (temperature: 25 ± 0.5 °C, humidity: 55 ± 5%, 12 h: 12 h light dark cycle), and access to water and standard laboratory diet ad libitum. All animal experiments were conducted in accordance with the Laboratory Care and Use Guidelines. The research was approved by Ethics Committee of the Chinese PLA General Hospital (Approval ID: IACUC-2021-0022).

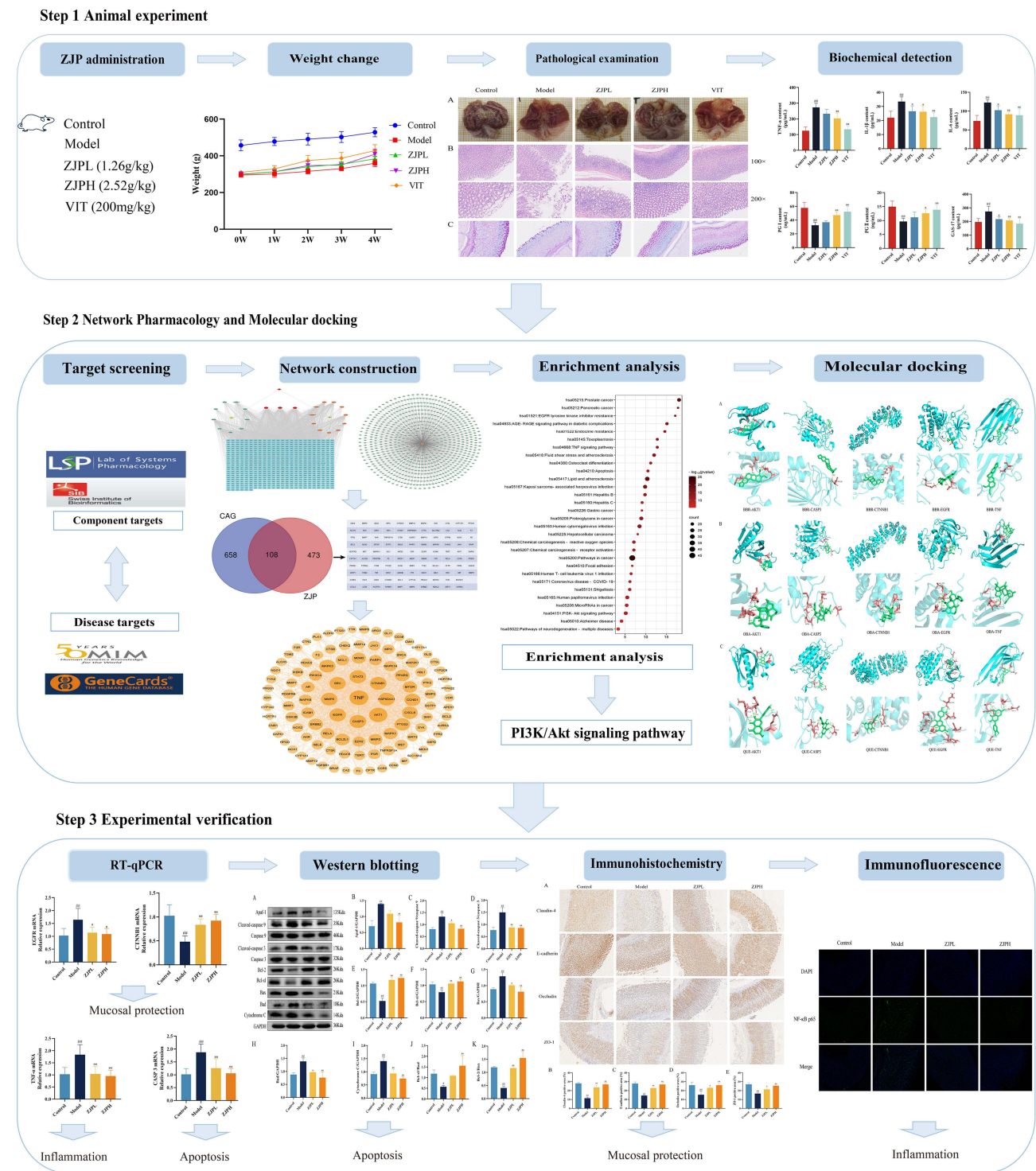


**Figure 1** Flow chart of this study. ZJPL: Zuojin Pill low dose (1.26g/kg); ZJPH: Zuojin Pill high dose (2.52g/kg); VIT: Vitacoenzyme (200 mg/kg). <sup>#</sup>P < 0.05 and <sup>###</sup>P < 0.01 vs control group. \*P < 0.05 and <sup>\*\*</sup>P < 0.01 vs model group.

After one week of quarantine and adaptation, 34 SD rats have randomly divided into 2 groups: 8 in control group and 26 in model group. CAG was established by a method as previously described.<sup>21</sup> Briefly, the rats in model group alternatively received 0.1% ammonia and 20 mmol/L sodium deoxycholate solution, accompanied with irregular fasting cycle. Ten weeks later, 2 rats in the control group and model group were randomly selected to detect the success of CAG modeling. All the rats with CAG were divided into four groups: model group, positive drug group (Vitacoenzyme, VIT,

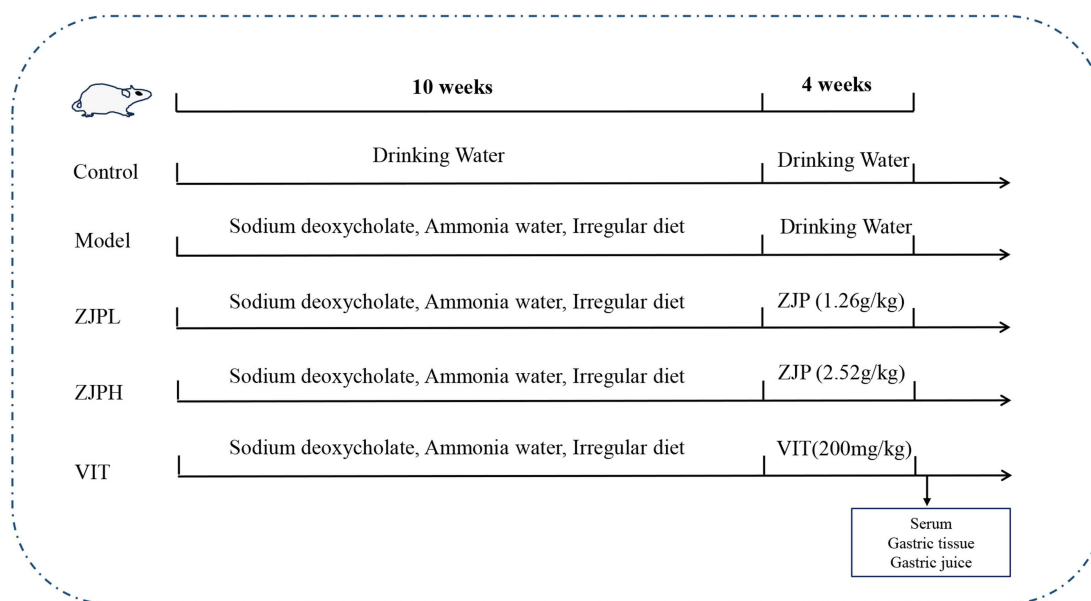


**Figure 2** The schematic overview of the experimental design.

**Abbreviations:** ZJPL, Zuojin Pill low dose (1.26g/kg); ZJPH, Zuojin Pill high dose (2.52g/kg); ZJP, Zuojin Pill; VIT, Vitacoenzyme (200 mg/kg).

200 mg/kg), ZJP low dose group (ZJPL, 1.26g/kg), ZJP high dose group (ZJPH, 2.52g/kg).<sup>22</sup> The corresponding drugs were given by intragastric administration for 4 weeks (Figure 2).

## Sample Collection

At the end of the experiment, all rats were fasted for 24 h with access to water. Firstly, rats were sacrificed under 20% ethyl carbamate solution. Secondly, blood samples were collected from the abdominal aorta and gastric tissues were removed. After centrifugation, the blood serum was stored at  $-80^{\circ}\text{C}$  until analysis. The gastric tissues were divided into two parts. One part was fixed in 10% paraformaldehyde for subsequent pathological examination and the other part was stored at  $-80^{\circ}\text{C}$  for subsequent molecular measurement. Finally, the gastric juice was collected and centrifuged at  $4^{\circ}\text{C}$  and 13,000 rpm for 10 min. The supernatant was taken and then subjected to PH determination.

## Pathological Observation

The gastric tissues were fixed in 10% neutral formalin solution and then dehydrated in ethanol and xylene respectively. After dehydration, the samples were embedded in paraffin wax.  $4\ \mu\text{m}$  thick serial slices were obtained and stained with hematoxylin and eosin (H&E) and Alcian blue-Periodic acid-Schiff (AB-PAS) staining. The histopathology of gastric mucosa was observed by Nikon microscope (Nikon instruments, Japan).

## Biochemical Detection

The serum biochemical levels of interleukin-6 (IL-6), interleukin- $1\beta$  (IL- $1\beta$ ), and tumor necrosis factor- $\alpha$  (TNF- $\alpha$ ) were measured following the manufacturer's instructions. Additionally, ELISA kits were used to quantify the levels of Pepsinogen I (PG I), Pepsinogen II (PG II), and Gastrin17 (GAS-17).

## TdT-Mediated dUTP Nick-End Labeling (TUNEL) Staining

The gastric tissues were fixed in paraformaldehyde prior to paraffin embedding, and then cut into  $4\ \mu\text{m}$  sections. Then, the TUNEL staining was used to evaluate the apoptosis rate as described previously.<sup>5</sup> The apoptosis of cells was observed under light microscope, and the results were expressed by the average number of TUNEL positive staining cells per  $200\times$  magnification.

## Measurement of Gastric PH

The accurate PH indicator paper was used to detect the PH value of gastric juice in each group after centrifugation.<sup>23</sup> And the same person used a colorimetric card to immediately read out the PH value for qualitative analysis.

## Data Preparation of Network Pharmacology

### Selection of Target Compounds for ZJP

The compounds of ZJP were collected using the Traditional Chinese Medicine Systems Pharmacology Database (TCMSP, <http://lsp.nwu.edu.cn/tcmsp.php>). Candidate compounds were screened according to the criteria of oral bioavailability (OB)  $\geq 30\%$  and drug-likeness (DL)  $\geq 0.18$ . Then, the targets of the candidate components of ZJP were screened in SwissTargetPrediction database (<http://www.swisstargetprediction.ch/>) (Probability $>0$ ). Finally, Cytoscape 3.8.0 software (Cytoscape Consortium, National Institute of General Medical Sciences, USA) was used to make the network diagram of “ZJP-compounds-targets”.

### Identification of CAG Targets

The CAG targets were obtained from the GeneCards (<http://www.genecards.org/>) and Online Mendelian Inheritance in Man (OMIM, <http://www.omim.org/>) databases with “chronic atrophic gastritis” or “CAG” as the keyword. By integrating these two databases, duplicate targets were removed and all targets were merged and standardized to construct a CAG disease target dataset. Finally, the network diagram of “CAG- target” was visualized by Cytoscape 3.8.0 software.

### Construction of Protein-Protein Interaction (PPI) Network

Venn diagram of CAG and ZJP targets was drawn by Venn online tool (<https://bioinformatics.psb.ugent.be/webtools/Venn/>) and intersection was taken. The PPI network was constructed through the String (<https://www.string-db.org/>) database and visualized using Cytoscape3.8.0 software.

### GO and KEGG Pathway Enrichment Analysis

Kyoto Encyclopedia of Genes and Genomes (KEGG) pathway enrichment analysis and Gene Ontology (GO) analysis were performed by linking targets to the Database for Annotation, Visualization and Integrated Discovery (DAVID, <https://david.ncifcrf.gov/>). GO terms and KEGG pathways with  $P$  value  $< 0.05$  were considered statistically significant. Finally, the top 20 KEGG pathways and the top 10 pathways of cell composition, biological process and molecular function in GO enrichment analysis were selected for visual analysis.

## Total RNA Extraction and Real-Time PCR

Total RNAs were extracted from gastric tissues with RNA extraction kit (Huaxingbio, Beijing, China), and then the mRNA was reverse transcribed into cDNA template for PCR amplification. RT-qPCR analysis was performed using SYBR Green PCR Master Mix (Huaxingbio, Beijing, China) and executed on 7500 Fast Real-Time PCR System (Applied Biosystems, Foster City, CA, USA). The data was calculated through  $2^{-\Delta\Delta CT}$  method with GAPDH as an endogenous reference. The primer sequences were listed in [Supplementary Table 1](#).

## Western Blotting Assay

The total protein of gastric tissues were extracted with ice-cold radioimmunoprecipitation assay (RIPA) buffer containing phenylmethylsulfonyl fluoride (PMSF) and the phosphatase inhibitor. The protein concentrations were determined by a BCA Protein Assay Kit. Protein samples were separated on sodium dodecyl sulphatepolyacrylamide gel electrophoresis (SDS-PAGE) and then transferred to polyvinylidene difluoride (PVDF) membranes. Next, the membranes were blocked for 2 h at room temperature. Then, all the membranes were incubated overnight at 4 °C with corresponding primary antibodies and the details were shown in [Supplementary Table 2](#). The next day, all membranes were washed 5 times with TBS-0.1% Tween 20 (TBST) and incubated with secondary antibody for 2 h at room temperature. Finally, the membranes were again washed 5 times with TBST and then visualized using ECL Plus detection kit. GAPDH as internal reference. The ImageJ software (National Institutes of Health, Bethesda, United States) was used for quantitative analysis of the acquired images.

## Immunohistochemistry

The gastric tissue samples were first fixed in a 10% formaldehyde solution, then embedded in paraffin and sliced. The tissue sections were dewaxed and rehydrated with graded ethanol. The antigen was extracted by citric acid antigen repair buffer (pH6.0) in microwave for 16 min. After natural cooling, the tissue was placed in phosphate buffered saline (PBS) with pH7.4 for 3 times for 5min. The tissues were incubated in darkness with 3% hydrogen peroxide solution at room temperature for 25 min, then 3% bovine serum albumin was dropped into the histochemical circle, uniformly covered the tissues, and sealed at room temperature for 30 min. Then, the samples were incubated with a primary rabbit polyclonal anti-ZO-1 antibody (Huaxingbio, HX19906, 1:100), rabbit polyclonal anti-Claudin-4 antibody (Huaxingbio, HX13369, 1:100), rabbit polyclonal anti-E-cadherin antibody (Huaxingbio, HX14050, 1:300) and rabbit polyclonal anti-Occludin antibody (Huaxingbio, HX20200, 1:300) at 4 °C overnight. The sections were then incubated with a horseradish peroxidase (HRP)-conjugated goat anti-rabbit secondary antibody (Huaxingbio, HX2031, 1:5000) and counterstained with hematoxylin. Images of three randomly chosen fields on each slide were captured under a microscope. The quantification of protein expression was presented with integrated optical density (IOD), using ImageJ software (National Institutes of Health, Bethesda, United States).

## Immunofluorescence

Paraffin sections of gastric tissues were dewaxed and dehydrated in graded ethanol, and placed in ethylenediaminetetraacetic acid (EDTA) for antigen retrieval. The sections were then washed three times with phosphate-buffered saline (PBS) and blocked for 30 min at room temperature with 1% BSA. Subsequently, the sections were incubated with anti-NF- $\kappa$ B p65 antibody overnight at 4°C. The next day, after incubating with the corresponding secondary antibody for 1 hour at room temperature and staining the nuclei with 4,6-diamino-2-phenylindole (DAPI), images were taken using a confocal microscope (NIKON Eclipse C1, Nikon Instruments Inc., Japan) and analyzed by NIKON DS-U3 (Nikon Instruments Inc., Japan). For quantitative analysis of the NF- $\kappa$ B p65 immunofluorescence staining, integral optical density (IOD) was measured by Image software.

## Molecular Docking

Molecular docking was performed after screening key targets and the key ingredients from the PPI network and the “key ingredients-targets” network of ZJP in treatment of CAG. The structure of the key targets was obtained from RCSB database (<https://www.rcsb.org/>) and the mol2 format files of key ingredients were downloaded from the TCMSP database. AutoDock Tools 1.5.6 was used for molecular docking, and PyMol software was used to visualize the molecular docking results.

## Statistical Analysis

Statistical analyses were performed with SPSS 26.0 (International Business Machines Corporation, New York, United States). All data were expressed as means  $\pm$  standard deviation (SD). Statistical differences between the groups were analyzed with a two-tailed Student's *t*-test or one-way analysis of variance (ANOVA). GraphPad Prism software (version 8.0) was used to visualize the results.  $P < 0.05$  was considered statistically significant.

## Results

### Evaluation of CAG Model Establishment

In order to verify whether the model is successful, the rats in the model group were tested after 10 weeks of continuous modeling. The results showed that the rats in the model group had slower weight gain, listlessness, less activity, messy fur and lack of luster. The gastric mucosa of the rats in the model group became thinner, the mucosal folds were reduced and flattened, the tissue lacked elasticity (Figure 3A). HE staining showed that there was loss of inherent glands, partial mucosal detachment, as well as neutrophil infiltration in the mucosa in the model rats (Figure 3B). Compared with the control group, the body weight of rats decreased significantly after modeling (Figure 3C).

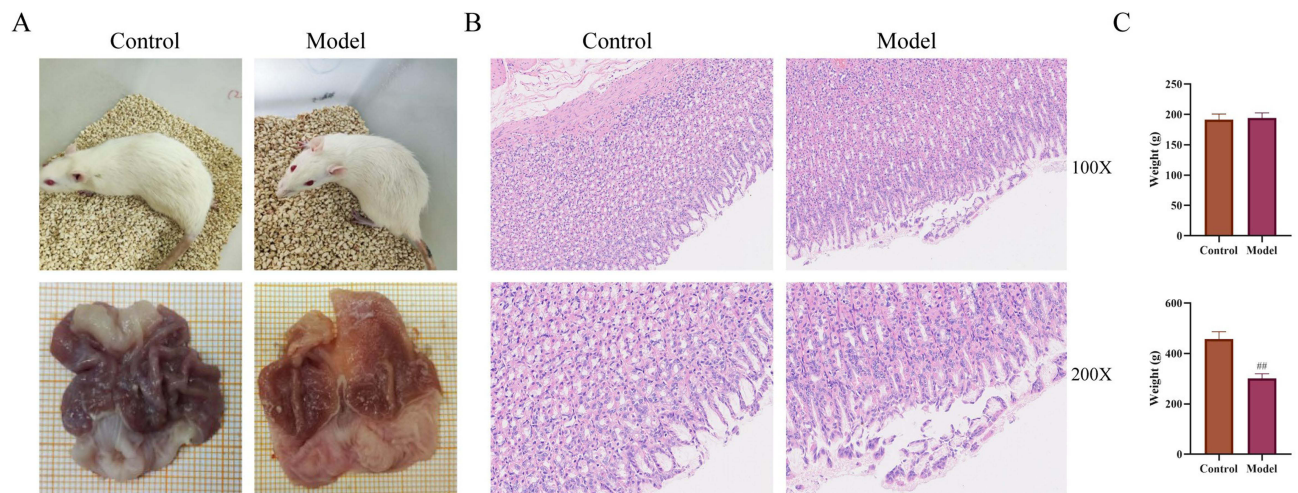


**Figure 3** Evaluation of CAG model establishment. **(A)** General state of rats and macroscopic manifestation of gastric tissue in the control and model group. **(B)** HE staining of gastric tissue in control group and model group. **(C)** Changes of body weight of rats in control group and model group. All data were expressed as means  $\pm$  standard deviation (SD). Two group comparisons were analyzed by unpaired two tailed Student's *t*-test. ##*P* < 0.01 vs control group.

## Effect of ZJP on General Condition and Body Weight in CAG Rats

The most typical feature of CAG is weight loss. With the increase of modeling time, the body weight of the model group was significantly lower than that of the control group. And the ZJP group and the vitacoenzyme group exerted well improvement on the body weight, indicating that they had similar therapeutic effect on CAG rats (Figure 4A). The pH values of gastric juice in model group were significantly higher than control group. ZJP had an excellent moderation effect on the pH of gastric juice (Figure 4B). In addition, the rats in the control group were in good condition with shiny fur and free movement, while the rats in model group presented pale yellow color hair, lack of energy, sleepiness, and

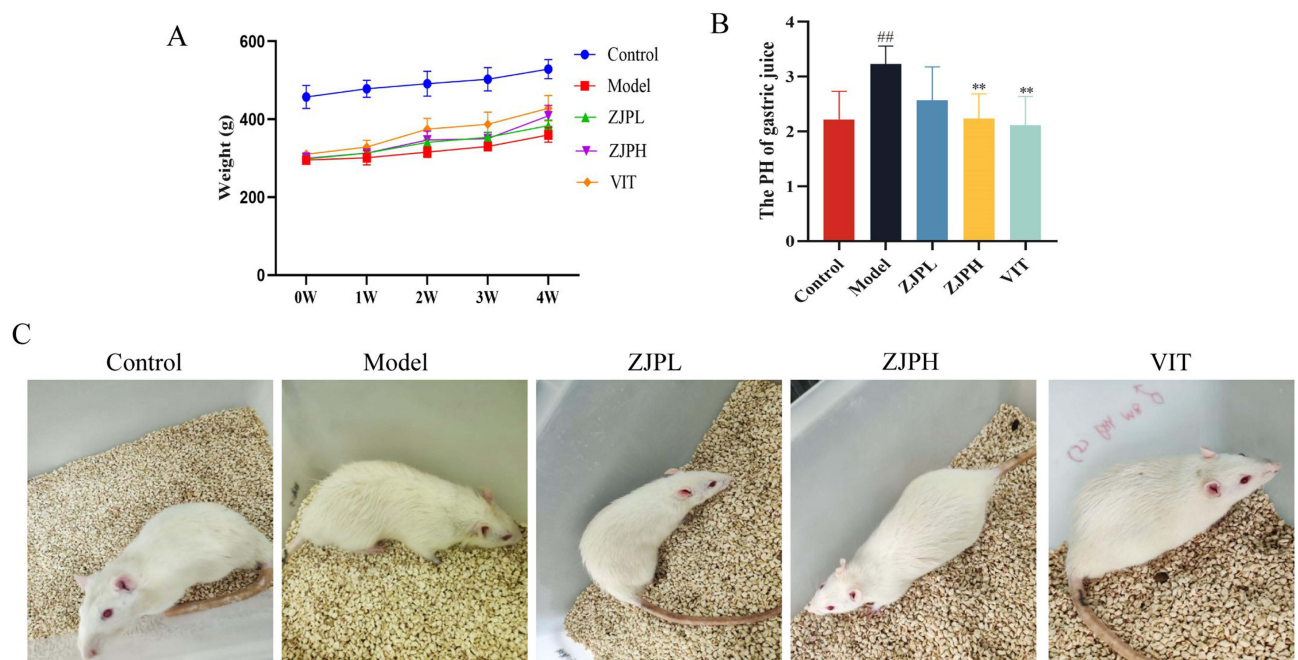


**Figure 4** Effect of ZJP on general condition and body weight. **(A)** Changes of body weight in each group. **(B)** The result of gastric juice pH test. **(C)** General state of rats in the groups. All data were expressed as means  $\pm$  standard deviation (SD). Multiple comparisons were analyzed by ANOVA. ##*P* < 0.01 vs control group. \*\**P* < 0.01 vs model group. **Abbreviations:** ZJPL, Zuojin Pill low dose (1.26g/kg); ZJPH, Zuojin Pill high dose (2.52g/kg); VIT, Vitacoenzyme (200 mg/kg).

decreased appetite. After treatment with ZJP and vitacoenzyme, the above symptoms in each group were alleviated to some extent. The improvement effect of ZJPH group was better than that of ZJPL group (Figure 4C).

## ZJP Attenuated the Pathological Changes of CAG Rats

Macroscopic and microscopic were applied to observe the integral morphology and pathological changes of gastric tissues, respectively. Macroscopic observation showed that the gastric tissue was thinner and the gastric fold was shallower in model group. The morphology of gastric mucosa of rats in the ZJPL, ZJPH and vitacoenzyme groups had deep wrinkles and rich mucosal layer (Figure 5A).

The pathological changes of gastric tissue were observed by HE staining. In the control group, the gastric mucosal cells and proper glands were neatly arranged and the structure was complete. In contrast, the gastric mucosa of the model group rats was atrophic and thin, the glands were significantly reduced, the arrangement was irregular, and the inflammatory cells infiltrated. Moreover, rats in the ZJPL, ZJPH group and the vitacoenzyme group showed orderly arrangement of gastric mucosal cells, reduced degree of glandular atrophy, relatively intact glandular structure, and less infiltration of inflammatory cells (Figure 5B). The thickness of functional gastric mucosa was characterized by AB-PAS staining. Compared with the control group, the thickness of gastric mucosa in the model group was significantly reduced, while the administration of ZJP and vitacoenzyme supplements improved the thickness of the mucosa to varying degrees (Figure 5C).

## ZJP Inhibited Inflammatory Response in CAG Rats

To characterize the inflammatory injury of CAG, inflammation-related factors including TNF- $\alpha$ , IL-1 $\beta$ , IL-6, and NF- $\kappa$ B p65 were detected. As shown in Figure 6A–C, the serum levels of TNF- $\alpha$ , IL-1 $\beta$  and IL-6 in the model group were

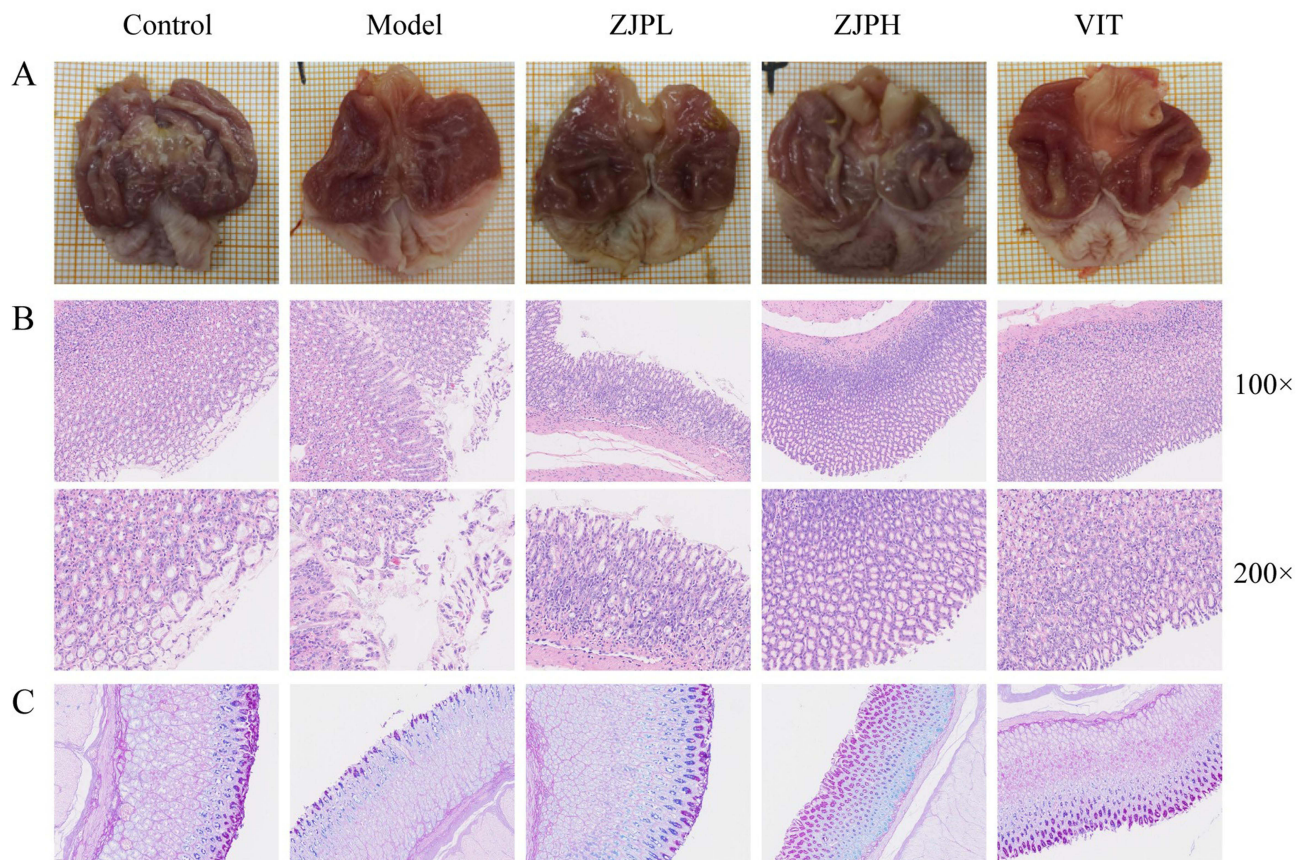


**Figure 5** Effect of ZJP on gastric mucosal injury. (A) Macroscopic morphology of each group. (B) HE staining of gastric histopathology. (C) Representative images AB-PAS staining of each group.

**Abbreviations:** ZJPL, Zuojin Pill low dose (1.26g/kg); ZJPH, Zuojin Pill high dose (2.52g/kg); VIT, Vitacoenzyme (200 mg/kg).



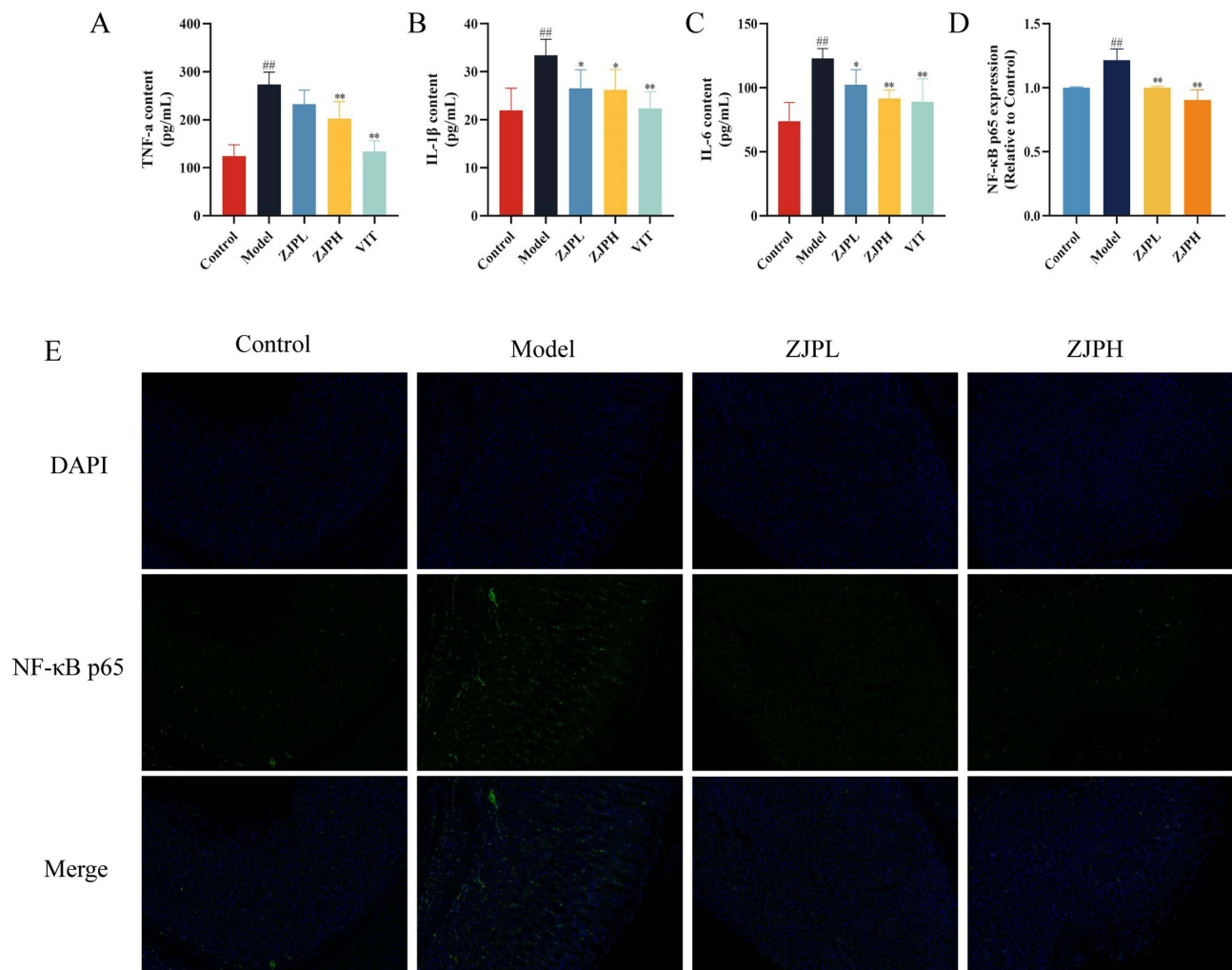


**Figure 6** Effect of ZJP on inflammatory response. **(A)** The expression level of TNF- $\alpha$  in serum. **(B)** The expression level of IL-1 $\beta$  in serum. **(C)** The expression level of IL-6 in serum (n=6). **(D)** The NF- $\kappa$ B p65 relative expression **(E)** Representative immunofluorescence staining images in gastric mucosa showing NF- $\kappa$ B p65 expressing (400 $\times$  magnification). All data were expressed as means  $\pm$  standard deviation (SD). Multiple comparisons were analyzed by ANOVA. ## $P$  < 0.01 vs control group. \* $P$  < 0.05 and \*\* $P$  < 0.01 vs model group.

**Abbreviations:** ZJPL, Zuojin Pill low dose (1.26g/kg); ZJPH, Zuojin Pill high dose (2.52g/kg); VIT, Vitacoenzyme (200 mg/kg).

notably higher than that in the control group. Compared with the model group, the expression of TNF- $\alpha$ , IL-1 $\beta$  and IL-6 of ZJP group were down-regulated in the ZJP group. In particular, the inhibition effect of ZJPH group was more obvious than that of ZJPL group. In addition, we also analyzed the expression of NF- $\kappa$ B p65 by immunofluorescence, and the results indicated that in the model group, there was a significant increase the expression of NF- $\kappa$ B p65. However, ZJP treatment significantly decreased the expression of NF- $\kappa$ B p65 in a dose-dependent manner, which indicated that ZJP improved the gastric injury by reducing the inflammatory reaction (Figure 6D and E).

## ZJP Improved Biomarkers in Serum of CAG Rats

To clarify the activities of several specific markers of CAG, the serum levels of PG I, PG II and GAS-17 were measured. As revealed in Figure 7A–C, the levels of PG I and PG II decreased markedly, and the level of GAS-17 increased significantly in model group compared to control group. Conversely, the above indexes reversed significantly after ZJP and vitacoenzyme administration, and the effect of ZJPH group was more obvious than that of ZJPL group.

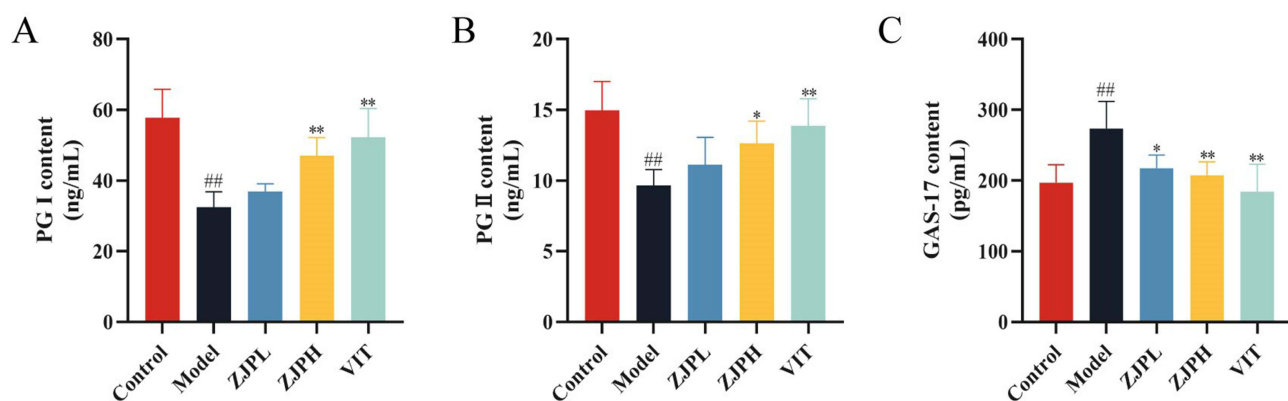


**Figure 7** Effect of ZJP on biomarkers in serum of CAG. **(A)** The expression level of PG I in serum. **(B)** The expression level of PG II in serum. **(C)** The expression level of GAS-17 in serum. (n=6) All data were expressed as means  $\pm$  standard deviation (SD). Multiple comparisons were analyzed by ANOVA. <sup>##</sup> $P < 0.01$  vs control group. <sup>\*</sup> $P < 0.05$  and <sup>\*\*</sup> $P < 0.01$  vs model group.

**Abbreviations:** ZJPL, Zuojin Pill low dose (1.26g/kg); ZJPH, Zuojin Pill high dose (2.52g/kg); VIT, Vitacoenzyme (200 mg/kg).

## Network Pharmacology and Molecular Docking Predicted Potential Mechanism for ZJP Treatment of CAG

### Potential Targets and Cross-Gene Screening of ZJP and CAG

We used network pharmacology technology to predict ZJP components and CAG targets, and obtained enriched signaling pathways, which provided directions for further molecular mechanism studies. A total of 33 compounds and 826 targets of ZJP and 766 targets of CAG related targets were identified after merging and removing duplicate genes (Figure 8A and B). As revealed in Figure 8C and D, 108 overlapped genes related to compounds and CAG were kept for PPI network construction using STRING database. Additionally, visualizing the PPI network through Cytoscape software, larger nodes represent higher degree values and are considered key targets. These key targets were associated with inflammation, apoptosis, and mucosal protection.

### GO and KEGG Enrichment Analysis and Construction of PPI Network

To clarify the biological functions and crucial pathways among the key targets in CAG treatment, GO and KEGG pathway enrichment analysis was performed. As shown in Figure 9A–D and Supplementary Tables 3 and 4, the top important 30 signaling pathways of the KEGG and the top 10 GO terms were significantly enriched. KEGG enrichment analysis showed that key target genes were strongly associated with PI3K/Akt signaling pathway, TNF signaling pathway and so on. Among them, the PI3K/Akt signaling pathway is the most significant pathway. The GO results suggest that the top 10 GO biological processes associated with ZJP treatment of CAG included negative regulation of apoptotic process, positive regulation of transcription from RNA polymerase II promoter, positive regulation of gene expression, signal transduction, and protein phosphorylation, etc; the associated cellular components included cytoplasm, nucleus, cytosol, plasma membrane, and nucleoplasm, etc; the related molecular functions included protein binding, identical protein binding, ATP binding, protein kinase activity, and enzyme binding, etc. Next, we structured the interaction network between the top important 30 signaling pathways and GO terms information collected in enrichment analysis and the relevant genes in each signaling pathway, which were concerned with the mechanism of ZJP in treating CAG.

### ZJP Regulated Key Genes in the Treatment of CAG

Network pharmacology have predicted that ZJP exerted the therapeutic effect on CAG mainly through inflammation, apoptosis, and mucosal protection. Therefore, we conducted experiments to verify these related targets. Compared with the control group, the mRNA levels of AKT1, TNF- $\alpha$ , CASP 3 and EGFR increased significantly, and the mRNA level of CTNNB1 decreased significantly in the model group. Conversely, different doses of ZJP administration significantly decreased the levels of AKT1, TNF- $\alpha$ , CASP 3 and EGFR, and significantly increased the level of CTNNB1 in a dose-dependent manner (Figure 10A–E).

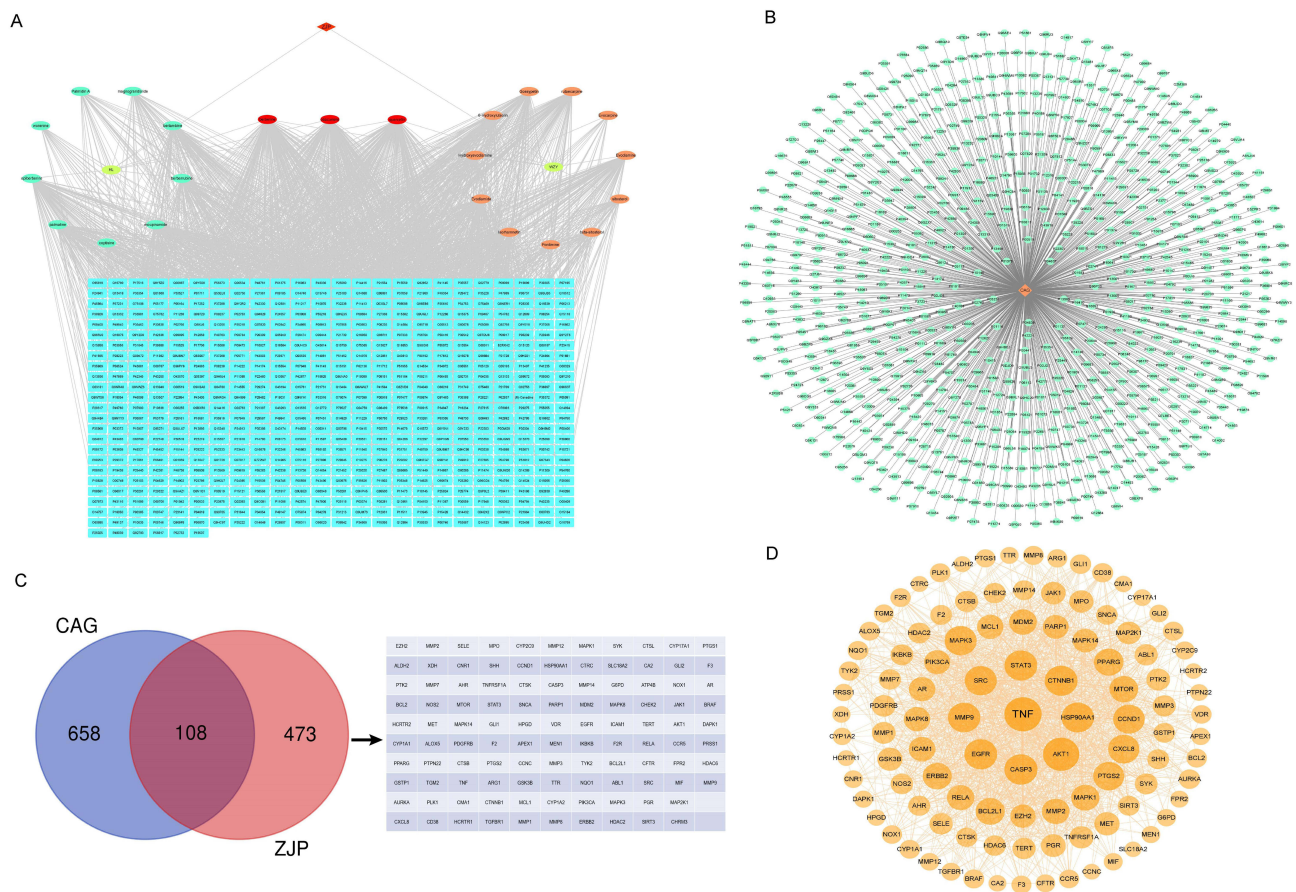


**Figure 8** Network pharmacology prediction for ZJP treatment of CAG. **(A)** “ZJP- ingredients- targets” network. **(B)** CAG related targets network. **(C)** Venn diagram. **(D)** The PPI network.  
**Abbreviations:** ZJP, Zuojin Pill; HL, Coptidis Rhizoma; WZY, Euodiae Fructus.

### ZJP Prevented CAG by Inhibiting PI3K/Akt Signaling Pathway

To verify the role of the PI3K-Akt signaling pathway in ZJP treatment of CAG, the protein expression levels of PI3K, Akt, and p-Akt in the gastric tissue were measured by Western blot analysis. As shown in Figure 11A–C, the expression levels of PI3K and p-Akt were increased in model group compared to the control group. In contrast to the model group, the protein expression of PI3K and p-Akt in each treatment group decreased significantly. There were no significant difference in the level of total Akt expression in the control group, model group and the ZJP groups. In addition, compared with the model group, p-Akt/Akt significantly reversed in a dose-dependent manner after ZJP treatment.

### ZJP Inhibited Apoptosis by Reducing Levels of Apoptosis-Related Proteins in CAG Rats

To further elucidate the anti-apoptotic effect of ZJP in the treatment of CAG, apoptotic-related proteins were detected. As shown in Figure 12A–K, the protein expressions of Bcl-2, Bcl-xl, and ratios of Bcl-2/Bax, Bcl-xl/Bad were dramatically reduced, and the Bax, Bad, Cytochrome C, cleaved-caspase-9, cleaved-caspase-3, and Apaf-1 protein expressions were significantly elevated compared with the control group. Conversely, after intragastric administration of ZJP, the abnormal expressions of Bcl-2, Bcl-xl, Bax, Bad, cleaved-caspase-9, cleaved-caspase-3, Apaf-1, Cytochrome C, ratios of Bcl-2/Bax, Bcl-xl/Bad were evidently reversed compared with the model group, which the effect was more pronounced in the ZJPH group. In addition, TUNEL staining was used to detect the effect of ZJP on the apoptosis level of gastric mucosa in rats. Compared to the model group, we detected a reduction of TUNEL-positive cells in gastric tissues after treatment with ZJP (Figure 12L).

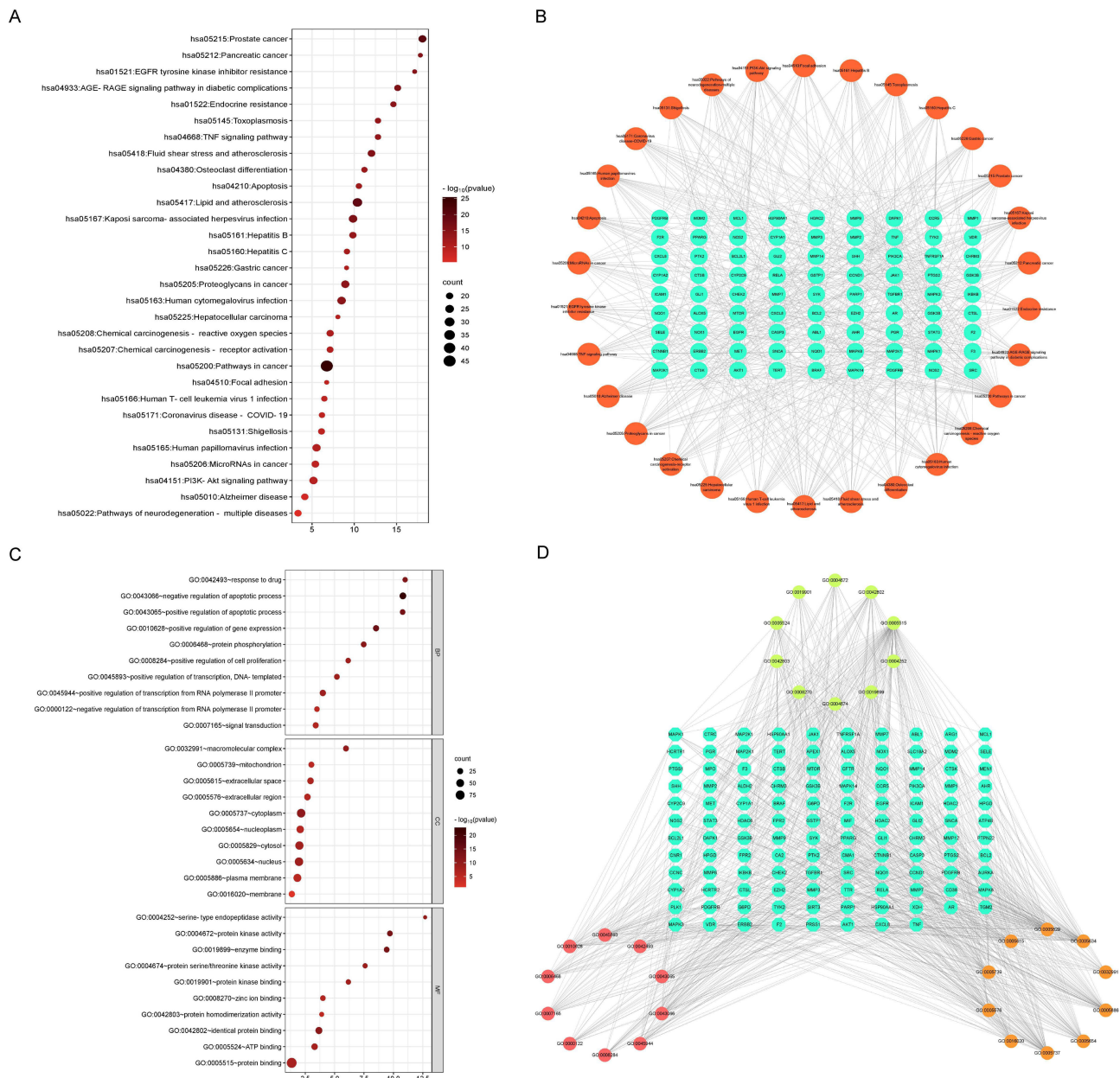


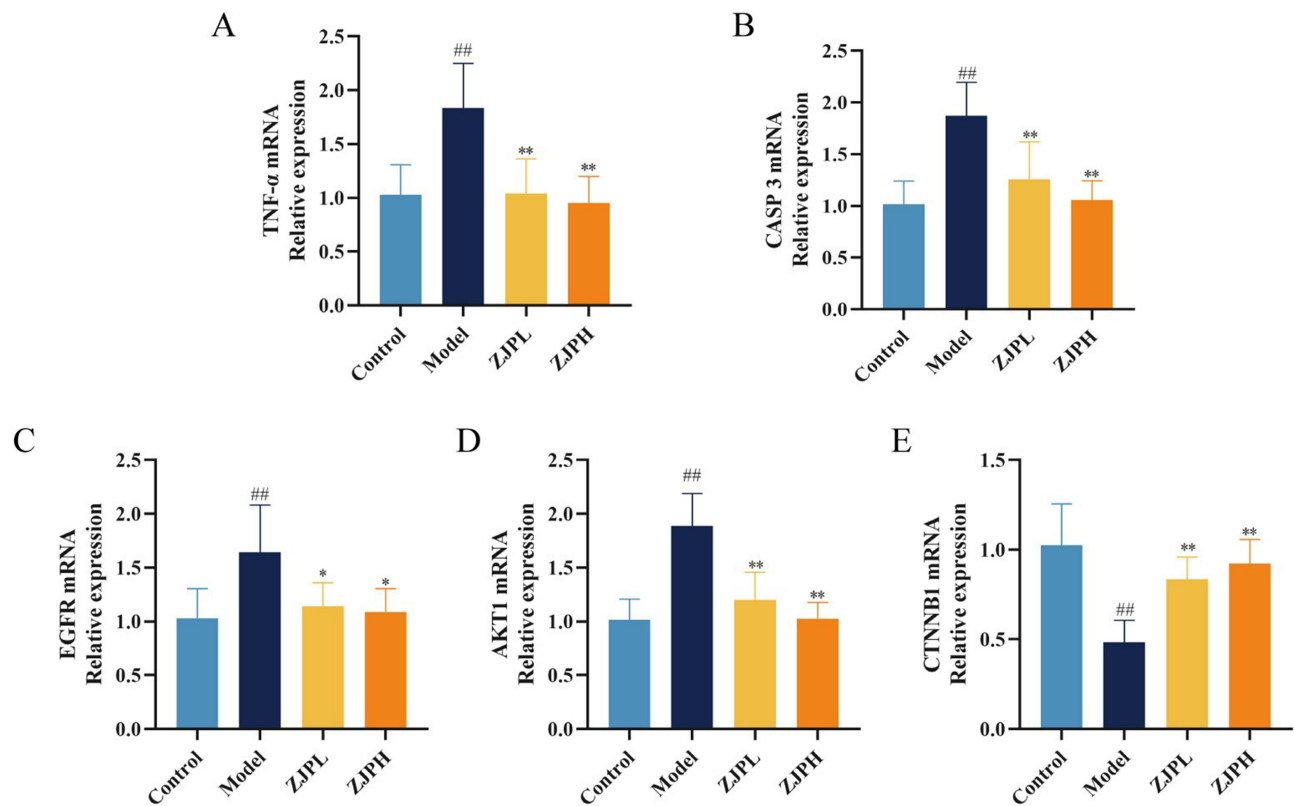
**Figure 9** Enrichment analysis and gene-pathway network analysis. (A) Top 30 KEGG terms of key genes. (B) Top 10 GO terms of key genes. (C) Gene-pathway network of ZJP in CAG. (D) Gene-GO terms network of ZJP in CAG.

## ZJP Protected the Integrity on Gastric Mucosa Epithelium

To further evaluated the protective effect of ZJP on the gastric mucosa of CAG rats, the protein expression of Occludin, ZO-1, Claudin-4 and E-cadherin were measured to evaluate the integrity on gastric mucosa epithelium. The results showed that the protein expression of Occludin, ZO-1, Claudin-4 and E-cadherin in the model group was significantly downregulated compared with the control group. In contrast, ZJP significantly reversed the proteins mentioned above. Especially in the ZJPH group. The results of mRNA expression were consistent with those of protein expression (Figure 13A–I).

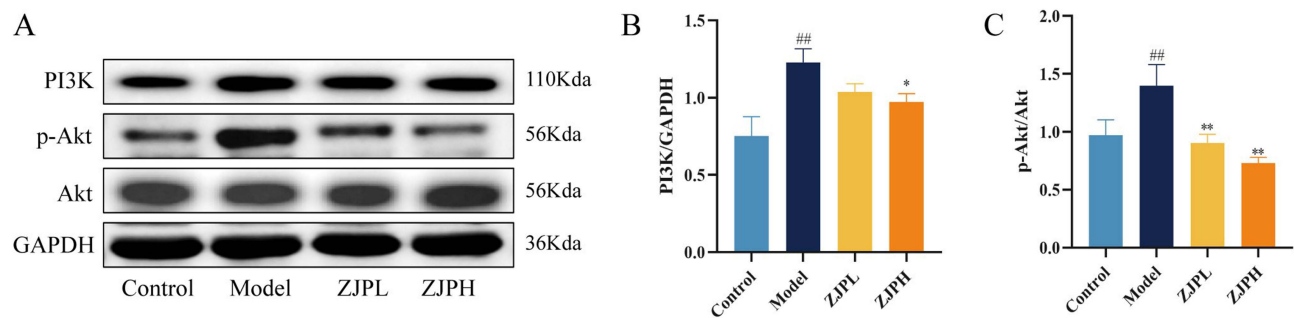
## Molecular Docking Analysis

To further explore the mechanism of ZJP in the treatment of CAG, the key targets and the key ingredients were selected for molecular docking. Based on the network pharmacology results, we screened the top 5 key targets, including TNF- $\alpha$ , EGFR,



**Figure 10** Effects of ZJP on key targets of CAG. **(A)** The TNF- $\alpha$  mRNA relative expression. **(B)** The CASP 3 mRNA relative expression. **(C)** The EGFR mRNA relative expression. **(D)** The AKT1 mRNA relative expression. **(E)** The CTNNB1 mRNA relative expression (n=6). All data were expressed as means  $\pm$  standard deviation (SD). Multiple comparisons were analyzed by ANOVA. ##*P* < 0.01 vs control group. \**P* < 0.05 and \*\**P* < 0.01 vs model group.

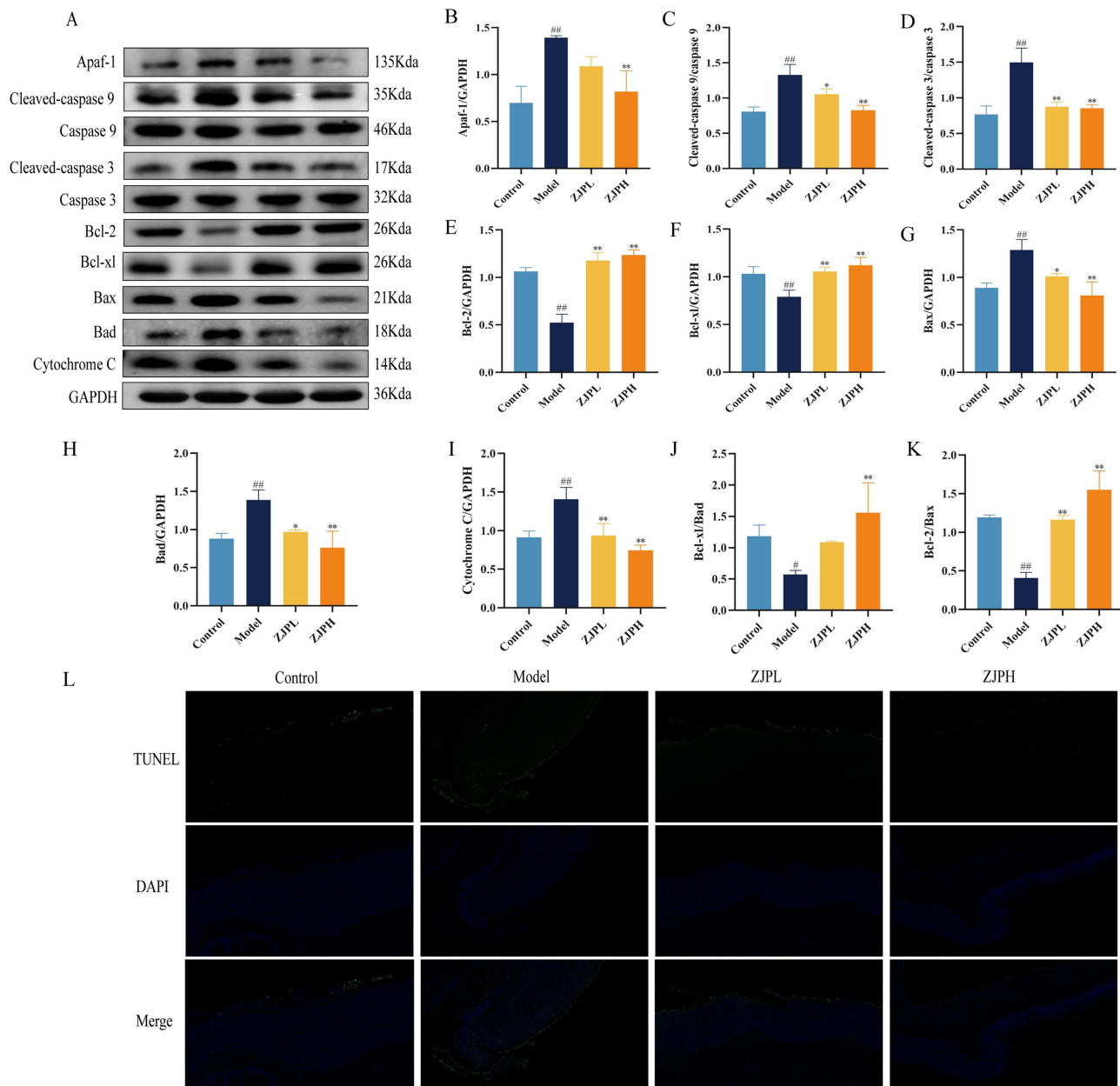
**Abbreviations:** ZJPL, Zuojin Pill low dose (1.26g/kg); ZJPH, Zuojin Pill high dose (2.52g/kg); VIT, Vitacoenzyme (200 mg/kg).



**Figure 11** Effects of ZJP on PI3K/Akt signaling pathway. **(A)** Western blotting images of PI3K, p-Akt and Akt. **(B)** The relative protein expression of PI3K. **(C)** Relative protein expression of p-Akt. All data were expressed as means  $\pm$  standard deviation (SD). Multiple comparisons were analyzed by ANOVA. ##*P* < 0.01 vs control group. \**P* < 0.05 and \*\**P* < 0.01 vs model group.

**Abbreviations:** ZJPL, Zuojin Pill low dose (1.26g/kg); ZJPH, Zuojin Pill high dose (2.52g/kg); VIT, Vitacoenzyme (200 mg/kg).

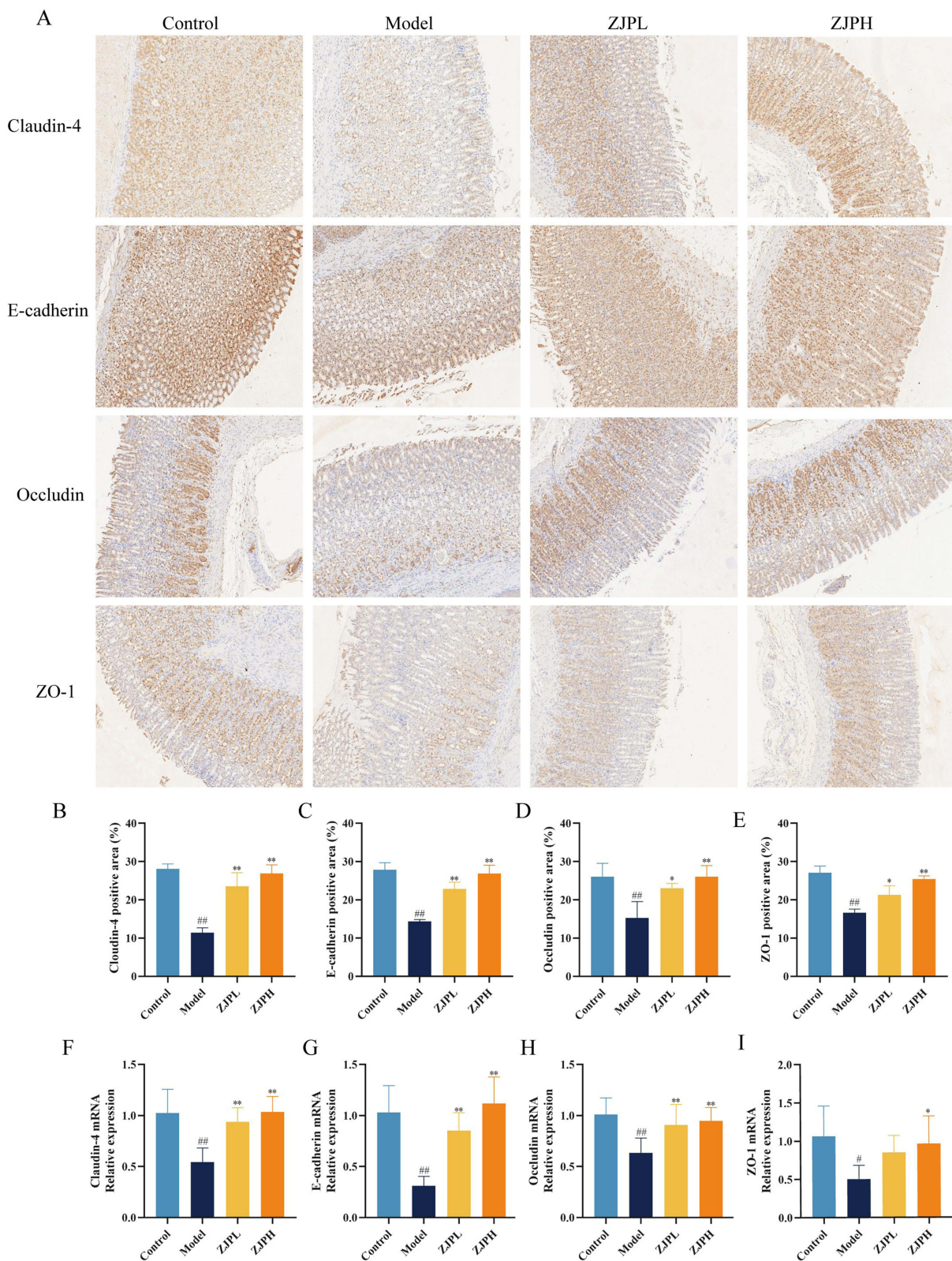
CASP 3, AKT1 and CTNNB1, and performed molecular docking with the top 3 key ingredients, including quercetin (QUE), obacunone (OBA) and berberine (BBR). The results showed that the PDB ID numbers of TNF, EGFR, CASP 3, AKT1 and CTNNB1 were 5UUI, 5Y9T, 5IBP, 1UNQ and 1JDH, respectively. The binding energy of most of these ingredients to the targets was less than  $-5$  kcal/mol, indicating a good binding activity and strong stability between the key ingredients and targets<sup>24</sup> (Table 1). In addition, Figure 14A–C exhibited an image of the optimal docking of ingredients and targets after visualization.



**Figure 12** Effects of ZJP on apoptosis-related proteins. **(A)** Western blotting images of apoptosis-related proteins. **(B)** The relative protein expression of Apaf-1. **(C)** The relative protein expression of cleaved-Caspase-9/ Caspase-9. **(D)** The relative protein expression of cleaved-caspase-3/Caspase-3. **(E)** The relative protein expression of Bcl-2. **(F)** The relative protein expression of Bcl-xl. **(G)** The relative protein expression of Bax. **(H)** The relative protein expression of Bad. **(I)** The relative protein expression of Cytochrome C. **(J)** The ratio of Bcl-xl/Bad. **(K)** The ratio of Bcl-2/Bax. **(L)** TUNEL analysis of apoptosis in the gastric tissues of rats in each group. All data were expressed as means  $\pm$  standard deviation (SD). Multiple comparisons were analyzed by ANOVA. ## $p < 0.05$  and ### $p < 0.01$  vs control group. \* $p < 0.05$  and \*\* $p < 0.01$  vs model group. **Abbreviations:** ZJPL, Zuojin Pill low dose (1.26g/kg); ZJPH, Zuojin Pill high dose (2.52g/kg); VIT, Vitacoenzyme (200 mg/kg).

## Discussion

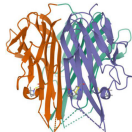
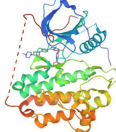
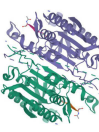
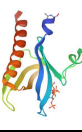

CAG is considered a characteristic precancerous lesion of gastric cancer with a high risk of developing into gastric cancer. In recent years, the incidence of CAG has increased and shown a trend towards younger onset, seriously affecting the health and quality of life of an increasing number of patients.<sup>25</sup> ZJP is a commonly used traditional Chinese prescription with a wide range of pharmacological actions in the digestive system.<sup>13</sup> An increasing number of studies have shown that ZJP has anti-inflammatory, antibacterial and mucosal protection effects.<sup>12,13,26</sup> With the continuous development of new technology, the mechanism of traditional Chinese medicine in treating CAG is becoming increasingly profound. In this study, the potential mechanism of ZJP in the treatment of CAG was explored by using the network



**Figure 13** Effects of ZJP on mucosal integrity. **(A)** The images of Occludin, ZO-1, Claudin-4 and E-cadherin in gastric tissues of rats was measured using immunohistochemical staining (100 ×). **(B)** Claudin-4 protein expression level. **(C)** E-cadherin protein expression level. **(D)** Occludin protein expression level. **(E)** ZO-1 protein expression level. **(F)** The Claudin-4 mRNA relative expression. **(G)** The E-cadherin mRNA relative expression. **(H)** The Occludin mRNA relative expression. **(I)** The ZO-1 mRNA relative expression. All data were expressed as means ± standard deviation (SD). Multiple comparisons were analyzed by ANOVA. <sup>#</sup>*P* < 0.05 and <sup>##</sup>*P* < 0.01 vs control group. <sup>\*</sup>*P* < 0.05 and <sup>\*\*</sup>*P* < 0.01 vs model group.

**Abbreviations:** ZJPL, Zuojin Pill low dose (1.26g/kg); ZJPH, Zuojin Pill high dose (2.52g/kg); VIT, Vitacoenzyme (200 mg/kg).

**Table I** Molecular Docking of Key Ingredients and Targets

Targets	PDB ID	Target Structure	Ingredients	Binding Energy (kcal/ mol)
TNF	5UUI		quercetin	-5.77
			obacunone	-6.95
			berberine	-6.73
EGFR	5Y9T		quercetin	-6.37
			obacunone	-8.04
			berberine	-7.45
CASP 3	5IBP		quercetin	-6.29
			obacunone	-7.15
			berberine	-6.49
AKT1	IUNQ		quercetin	-6.13
			obacunone	-7.03
			berberine	-6.47
CTNNB1	IJDH		quercetin	-4.26
			obacunone	-6.19
			berberine	-5.69

pharmacology combined with experimental verification. The data demonstrated that ZJP exerts a good therapeutic effect on CAG by inhibiting apoptosis and inflammatory response, improving gastric mucosal damage through the PI3K/Akt signaling pathway, which provided a certain theoretical basis for the study of ZJP in the treatment of CAG (Figure 15).

It was found that weight loss is typical clinical feature of CAG. In this study, the body weight of rats in model group decreased significantly, which could be significantly improved after administration of ZJP. In addition, pepsinogen (PG) is a proenzyme secreted by gastric mucosal cells, which exists in the human body in two forms: PG I and PG II. The changes in serum levels of PG I and PG II are effective indicators for reflecting the morphology and function of gastric mucosa.<sup>27–29</sup> It has been well-documented PGI and PGII are low levels in the CAG model group.<sup>30</sup> Last but not least, GAS-17 is a peptide hormone that participates in the division, proliferation, and apoptosis of gastrointestinal mucosal cells and the secretion of gastric acid. It can indicate the status of gastric mucosal function in the body, and its level is closely related to the occurrence and development of gastric diseases.<sup>31,32</sup> Therefore, comprehensive testing of PG I, PG II, and GAS-17 results can more comprehensively and accurately detect the status of CAG.<sup>33</sup> In our study, the results revealed that ZJP treatment upregulated expression of PG I, PG II, and GAS-17. Therefore, our results provide evidence for ZJP in the treatment of CAG.

Previous studies have shown that the production of pro-inflammatory cytokines in gastric mucosa exacerbates inflammation, and excessive production of these cytokines is the cause of gastric mucosal injury.<sup>34</sup> Multiple studies have confirmed that overexpression of cytokines has been shown to increase the risk of CAG in both animal and human models, with several key cytokines including TNF- $\alpha$ , IL-6, and IL-1 $\beta$ .<sup>16,35,36</sup> Notably, TNF- $\alpha$  generated is considered to be one of the most harmful cytokines involved in CAG.<sup>37</sup> IL-1 $\beta$  is a typical pro-inflammatory cytokine that activates specific immune responses and plays an immune surveillance role.<sup>38</sup> Additionally, IL-6 is a multifunctional pro-inflammatory cytokine produced by various cells. It plays a crucial role in immune regulation, inflammatory response, and tumor development.<sup>39</sup> NF- $\kappa$ B is a major redox-sensitive transcription factor that can induce the expression of various pro-inflammatory genes and regulate the expression of inflammatory cytokines.<sup>40</sup> Studies have found that inactivation of



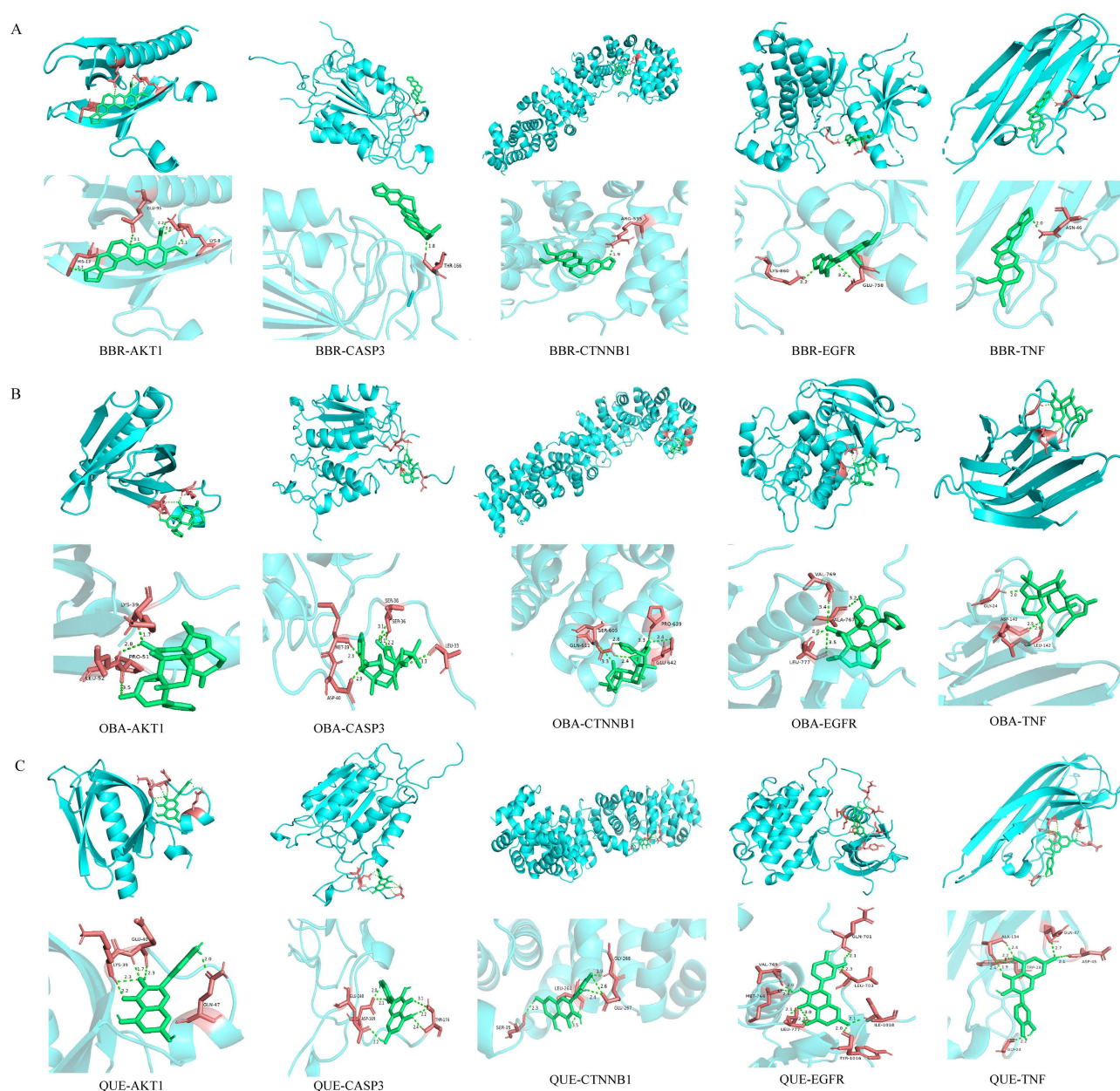


**Figure 14** Docking complexes 3D diagram of 5 key targets along with 3 key ingredients. **(A)** 3D binding posture schematic diagram of berberine and 5 key targets. **(B)** 3D binding posture schematic diagram of obacunone and 5 key targets. **(C)** 3D binding posture schematic diagram of quercetin and 5 key targets.

NF- $\kappa$ B lead to decreased expression of inflammatory cytokines such as TNF- $\alpha$ , IL-6, and IL-1 $\beta$ .<sup>41,42</sup> Our results suggested that ZJP could significantly inhibit the expression of TNF- $\alpha$ , IL-6, IL-1 $\beta$ , and NF- $\kappa$ B p65, with better effects observed in the ZJPH group. The above results indicate that ZJP exerts its therapeutic effect on CAG by inhibiting the inflammatory response.

Network pharmacology explains the biological network in which drugs play their role from the perspective of macro or global regulation, and provides new research ideas and technical means for studying the mechanism of action of TCM and TCM prescriptions.<sup>43</sup> In the present study, a network pharmacology approach was applied to identify active compounds, corresponding targets, and pharmacological mechanisms of ZJP in the treatment of CAG. The PI3K/Akt signaling pathway was considered an important pathway involved in the treatment of CAG, which exerted therapeutic effects through anti-inflammatory action, inhibition of apoptosis, and protection of gastric mucosa. The PI3K/Akt signaling pathway not only regulates apoptosis, migration, differentiation and metabolism of cells, but also plays

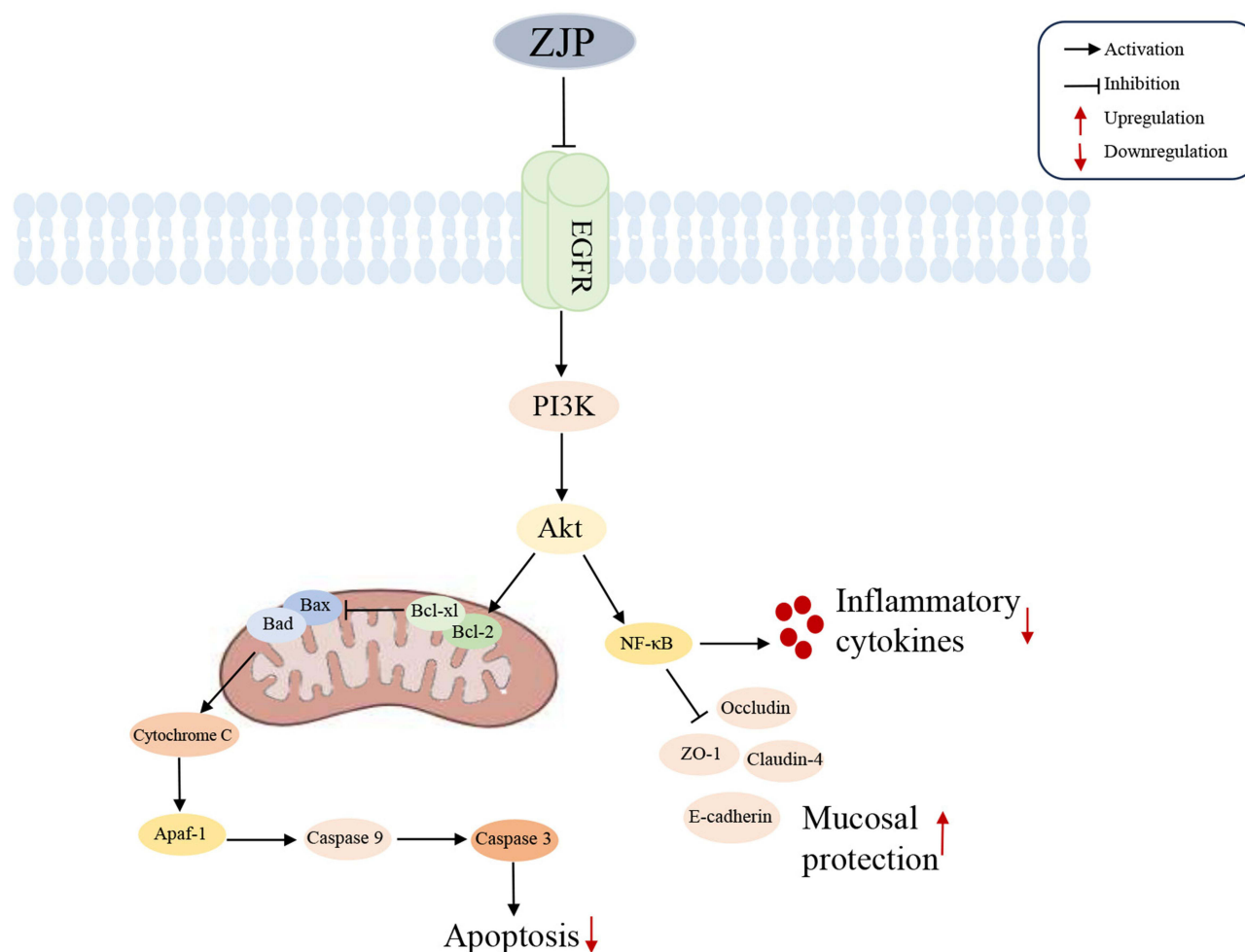


**Figure 15** Potential molecular mechanism of ZJP in the treatment of CAG.

a role in the reconstruction of gastric mucosa epithelium and promotes the occurrence and development of gastric tumors.<sup>44</sup> Studies have found that epidermal growth factor receptor (EGFR) can activate the expression of the PI3K signaling pathway.<sup>45,46</sup> Akt is a serine/threonine protein kinase located downstream of PI3K in the intracellular signal transduction system. Phosphorylation of Akt activates its kinase activity, leading to downstream molecular phosphorylation and regulation of cell apoptosis and inflammatory response.<sup>47–49</sup> In our study, ZJP improved CAG through PI3K/Akt signaling pathway, mainly by significantly reducing the ratio of p-Akt/Akt and the level of PI3K.

It has been reported that mitochondria is considered to be regulatory centers of biological energy, metabolism, and apoptosis, which is closely regulated by a variety of internal and external signals, including chemicals, Bcl-2, and caspase families etc.<sup>50</sup> In general, the mitochondrial apoptosis process is tightly regulated by the proteins of the Bcl-2 family, including anti-apoptotic proteins (Bcl-2 and Bcl-x1) and pro-apoptotic proteins (Bax and Bad).<sup>51</sup> The relative balance between anti-apoptotic proteins and pro-apoptotic proteins directly affects the physiological function of mitochondria.<sup>52,53</sup> It is well-known that activated Akt can phosphorylate the Ser136 residue of Bad, reducing the binding with Bcl-x1 and Bcl-2, thus playing a role in inhibiting apoptosis.<sup>54</sup> In addition, the pro-apoptotic protein induces apoptosis by disrupting the integrity of the mitochondrial membrane, causing a decrease in mitochondrial membrane potential and biochemical changes between the inner and outer mitochondrial membranes, ultimately resulting in the release of cytochrome c from the mitochondria into the cytoplasm. Subsequently, Apaf-1 is activated to form an apoptosome, which then activates caspase-3, triggering cell apoptosis.<sup>55,56</sup> Caspases are another family of enzymes, also known as aspartate-specific cysteine proteases, which play an important role in regulating the apoptotic signaling

pathway. Caspase9 is the promoter of Caspase in mitochondrial pathway, which is recruited and activated by apoptotic complex and activates downstream efferent protein Caspase 3 in turn, ultimately leading to cell apoptosis.<sup>51,57</sup> In the present study, we found that ZJP dramatically reduced the concentration of Cytochrome c in the cytosol, Bax, Bad, cleaved-caspase-9, cleaved-caspase-3 and Apaf-1 protein expressions and significantly elevated the protein expressions of Bcl-2, Bcl-xl, concentration of Cytochrome c in the mitochondria, and ratios of Bcl-2/Bax, Bcl-xl/Bad. These findings indicated that the therapeutic effect of ZJP on CAG was closely connected with inhibiting apoptosis.

The gastric mucosal barrier is an important defense mechanism that protects the body against pathogen invasion and maintains gastric homeostasis. Once it is compromised, it can lead to the occurrence and development of gastric diseases.<sup>58,59</sup> Cell junction is one of the main structures of gastric mucosal barrier, and tight junction is the most important membrane protein complex of cell junction, which is composed of occludin, claudin, ZO and junction adhesion molecule (JAM).<sup>60</sup> It is generally known that ZO-1 is a scaffold protein of the tight junction and is often used as an index to evaluate barrier function and permeability function.<sup>61</sup> In addition, occludin is an integral transmembrane protein at tight junctions, and increasing its concentration would enhance cell-to-cell adhesion.<sup>62</sup> Interestingly, in view of the evidence that claudin-4 can enrich occludin and interact with ZO-1. In addition, the expression of claudin-4 is closely related to gastric cancer.<sup>63</sup> Furthermore, E-cadherin has been previously reported to mediate cell adhesion and maintain the integrity of the organizational structure.<sup>64</sup> In our study, the expression of ZO-1, E-cadherin and occludin were significantly decreased, while the expression of claudin-4 was significantly increased in the model group, suggesting that CAG breached the mucosal layer and increased the permeability of gastric mucosa. However, ZJP reversed the expression of ZO-1, E-cadherin, claudin-4 and occludin, indicating that ZJP could protect the gastric mucosal barrier.

Although this study clarified the therapeutic efficacy of ZJP on CAG through integrated biological approach and explained the molecular biological mechanism of ZJP's improvement of CAG through PI3K/Akt signaling pathway, there are still some limitations in this study. For example, the effect of ingredients of ZJP on CAG has not been verified in this study; Although this study revealed that ZJP inhibits apoptosis and improves inflammation and gastric mucosal barrier through PI3K/Akt signaling pathway, there has been no reverse validation conducted for PI3K/Akt signaling inhibitors or activators in this experiment. Therefore, we will further enrich and refine this study in the future to comprehensively and systematically elucidate the molecular mechanisms and substance basis of ZJP in treating CAG, providing a research foundation for the rational clinical application of ZJP.

## Conclusion

In conclusion, our results demonstrated that ZJP exerted a therapeutic effect on CAG by regulating gastric mucosal barrier, suppressing inflammation, inhibiting apoptosis through PI3K/Akt signaling pathway. This study provided a methodological and theoretical basis for further revealing the pharmacological mechanism of ZJP in the treatment of CAG.

## Abbreviations

ZJP, Zuojin Pill; IL-6, Interleukin-6; CAG, Chronic atrophic gastritis; IL-1 $\beta$ , Interleukin-1 $\beta$ ; TCM, Traditional Chinese medicine; TNF- $\alpha$ , Tumor necrosis factor- $\alpha$ ; PG I, Pepsinogen I; OB, Oral bioavailability; PG II, Pepsinogen II; DL, Drug-likeness; GAS-17, Gastrin17; RIPA, Radioimmunoprecipitation assay; KEGG, Kyoto Encyclopedia of Genes and Genomes; PMSF, Phenylmethylsulfonyl fluoride; GO, Gene Ontology.

## Ethics Statement

All animal experiments were conducted in accordance with the Laboratory Care and Use Guidelines. The research was approved by Ethics Committee of the Chinese PLA General Hospital (Approval ID: IACUC-2021-0022).

## Acknowledgments

This research was financially supported by the Major Program of the National Natural Science Foundation of China (No. 82192915), the National Key Research and Development Program (No. 2018YFC1704500) and the China Postdoctoral Science Foundation (No. 2023M730115).

## Author Contributions

All authors made a significant contribution to the work reported, whether that is in the conception, study design, execution, acquisition of data, analysis and interpretation, or in all these areas; took part in drafting, revising or critically reviewing the article; gave final approval of the version to be published; have agreed on the journal to which the article has been submitted; and agree to be accountable for all aspects of the work.

## Disclosure

The authors declare that they have no competing interests in this work.

## References

1. Jayavelu ND, Bar NS. Metabolomic studies of human gastric cancer: review [J]. *World J Gastroenterol*. 2014;20(25):8092–8101. doi:10.3748/wjg.v20.i25.8092
2. Vannella L, Lahner E, Annibale B. Risk for gastric neoplasias in patients with chronic atrophic gastritis: a critical reappraisal [J]. *World J Gastroenterol*. 2012;18(12):1279–1285. doi:10.3748/wjg.v18.i12.1279
3. Bray F, Ferlay J, Soerjomataram I, et al. Global cancer statistics 2018: globocan estimates of incidence and mortality worldwide for 36 cancers in 185 countries [J]. *CA Cancer J Clin*. 2018;68(6):394–424. doi:10.3322/caac.21492
4. Zhenyukh O, Civantos E, Ruiz-Ortega M, et al. High concentration of branched-chain amino acids promotes oxidative stress, inflammation and migration of human peripheral blood mononuclear cells via mtorc1 activation [J]. *Free Radic Biol Med*. 2017;104:165–177. doi:10.1016/j.freeradbiomed.2017.01.009
5. Han L, Li T, Wang Y, et al. Weierning, a Chinese patent medicine, improves chronic atrophic gastritis with intestinal metaplasia [J]. *J Ethnopharmacol*. 2023;309:116345. doi:10.1016/j.jep.2023.116345
6. Li Z, Wu C, Li L, et al. Effect of long-term proton pump inhibitor administration on gastric mucosal atrophy: a meta-analysis [J]. *Saudi J Gastroenterol*. 2017;23(4):222–228. doi:10.4103/sjg.SJG\_573\_16
7. Donzelli A. Helicobacter pylori eradication? *Gastroenterology*. 2016;151(4):773–774. doi:10.1053/j.gastro.2016.05.059
8. Nazari M, Taghizadeh A, Orafaei H, et al. Nausea and vomiting in Iranian traditional medicine based on avicenna's viewpoint. *Elect Phys*. 2015;7(2):1047–1053. doi:10.14661/2015.1047-1053
9. Hamidpour R, Hamidpour M, Hamidpour S, et al. Cinnamon from the selection of traditional applications to its novel effects on the inhibition of angiogenesis in cancer cells and prevention of Alzheimer's disease, and a series of functions such as antioxidant, anticholesterol, antidiabetes, antibacterial, antifungal, nematocidal, acaracidal, and repellent activities. *J Traditional Complementary Med*. 2015;5(2):66–70. doi:10.1016/j.jtcm.2014.11.008
10. Liang F, Cooper EL, Wang H, et al. Acupuncture and immunity. *Evid Based Complement Alternat Med*. 2015;2015:260620. doi:10.1155/2015/260620
11. El Khoury D, Cuda C, Luhovyy BL, et al. Beta glucan: health benefits in obesity and metabolic syndrome. *J Nutr Metab*. 2012;2012:851362. doi:10.1155/2012/851362
12. Wei Y, Wang R, Ren S, et al. Zuojin pill ameliorates inflammation in indomethacin-induced gastric injury via inhibition of MAPK pathway [J]. *J Ethnopharmacol*. 2021;275:114103. doi:10.1016/j.jep.2021.114103
13. Wen J, Wu S, Ma X, et al. Zuojin pill attenuates helicobacter pylori-induced chronic atrophic gastritis in rats and improves gastric epithelial cells function in ges-1 cells. *J Ethnopharmacol*. 2022;285:114855. doi:10.1016/j.jep.2021.114855
14. Peng QX, Cai HB, Peng JL, et al. Extract of zuojin pill ([characters: see text]) induces apoptosis of sgc-7901 cells via mitochondria-dependent pathway. *Chin J Integr Med*. 2015;21(11):837–845. doi:10.1007/s11655-015-2043-3
15. Wang QS, Zhu XN, Jiang HL, et al. Protective effects of alginate-chitosan microspheres loaded with alkaloids from *coptis chinensis* franch. And *evodia rutaecarpa* (juss.) benth. (zuojin pill) against ethanol-induced acute gastric mucosal injury in rats. *Drug Des Devel Ther*. 2015;9:6151–6165. doi:10.2147/DDDT.S96056
16. Ma X, Xie S, Wang R, et al. Metabolomics profiles associated with the treatment of zuojin pill on patients with chronic nonatrophic gastritis. *Front Pharmacol*. 2022;13:898680. doi:10.3389/fphar.2022.898680
17. Li S, Zhang B. Traditional Chinese medicine network pharmacology: theory, methodology and application. *Chinese J Nat Med*. 2013;11(2):110–120. doi:10.1016/S1875-5364(13)60037-0
18. Li Q, Lan T, He S, et al. A network pharmacology-based approach to explore the active ingredients and molecular mechanism of lei-gong-gen formula granule on a spontaneously hypertensive rat model. *Chin Med*. 2021;16(1):99. doi:10.1186/s13020-021-00507-1
19. Xiang SY, Zhao J, Lu Y, et al. Network pharmacology-based identification for therapeutic mechanism of ling-gui-zhu-gan decoction in the metabolic syndrome induced by antipsychotic drugs. *Comput Biol Med* 2019;110:1–7. doi:10.1016/j.combiomed.2019.05.007
20. Guo W, Huang J, Wang N, et al. Integrating network pharmacology and pharmacological evaluation for deciphering the action mechanism of herbal formula zuojin pill in suppressing hepatocellular carcinoma. *Front Pharmacol*. 2019;10:1185. doi:10.3389/fphar.2019.01185
21. Cui J, Liu Y, Hu Y, et al. NMR-based metabolomics and correlation analysis reveal potential biomarkers associated with chronic atrophic gastritis. *J Pharm Biomed Anal*. 2017;132:77–86. doi:10.1016/j.jpba.2016.09.044
22. Tong Y, Wang R, Liu X, et al. Zuojin pill ameliorates chronic atrophic gastritis induced by mnng through tgf-beta1/pi3k/akt axis. *J Ethnopharmacol*. 2021;271:113893. doi:10.1016/j.jep.2021.113893
23. Kangwan N, Pintha K, Lekawanvijit S, et al. Rosmarinic acid enriched fraction from *perilla frutescens* leaves strongly protects indomethacin-induced gastric ulcer in rats. *Biomed Res Int* 2019;2019:9514703. doi:10.1155/2019/9514703
24. Hu Y, Liu T, Zheng G, et al. Mechanism exploration of 6-gingerol in the treatment of atherosclerosis based on network pharmacology, molecular docking and experimental validation. *Phytomedicine*. 2023;115:154835. doi:10.1016/j.phymed.2023.154835

25. Sun Y, Wang S, Qi M, et al. Psychological distress in patients with chronic atrophic gastritis: the risk factors, protection factors, and cumulative effect. *Psychol Health Med*. 2018;23(7):797–803. doi:10.1080/13548506.2018.1428756
26. Wang J, Zhang T, Zhu L, et al. Anti-ulcerogenic effect of zuojin pill against ethanol-induced acute gastric lesion in animal models. *J Ethnopharmacol*. 2015;173:459–467. doi:10.1016/j.jep.2015.04.017
27. Guo K, Li Z, Qiu B, et al. Analysis of gastric diseases and their symptoms based on indexes of pepsinogen i (pgi) and pepsinogen ii (pgii): take 1106 patients as samples. *Cellular Microbiology*. 2022;2022:1–6. doi:10.1155/2022/8393351
28. Cuomo P, Papaiani M, Capparelli R, et al. The role of formyl peptide receptors in permanent and low-grade inflammation: helicobacter pylori infection as a model. *Int J Mol Sci*. 2021;22(7):3706.
29. Booth AL, Gonzalez RS. Helicobacter pylori colonisation of duodenal foveolar metaplasia requires concurrent gastric infection. *J Clin Pathol*. 2021;74(8):537–539. doi:10.1136/jclinpath-2020-206844
30. Chen X, Zhang J, Wang R, et al. UPLC-Q-TOF/MS-based serum and urine metabolomics study on the ameliorative effects of palmatine on helicobacter pylori-induced chronic atrophic gastritis. *Front Pharmacol*. 2020;11:586954. doi:10.3389/fphar.2020.586954
31. Koivurova OP, Koskela R, Blomster T, et al. Serological biomarker panel in diagnosis of atrophic gastritis and helicobacter pylori infection in gastroscopy referral patients: clinical validation of the new-generation gastropanel<sup>®</sup> test. *Anticancer Res*. 2021;41(11):5527–5537. doi:10.21873/anticancer.15366
32. Kim YJ, Chung WC, Kim DB. Efficacy of bismuth added to standard triple therapy as the first-line eradication regimen for helicobacter pylori infection. *Helicobacter*. 2021;26(3):e12792. doi:10.1111/hel.12792
33. Zagari RM, Rabitti S, Greenwood DC, et al. Systematic review with meta-analysis: diagnostic performance of the combination of pepsinogen, gastrin-17 and anti-helicobacter pylori antibodies serum assays for the diagnosis of atrophic gastritis. *Aliment Pharmacol Ther*. 2017;46(7):657–667. doi:10.1111/apt.14248
34. Antonisamy P, Arasu MV, Dhanasekaran M, et al. Protective effects of trigonelline against indomethacin-induced gastric ulcer in rats and potential underlying mechanisms. *Food Funct*. 2016;7(1):398–408. doi:10.1039/C5FO00403A
35. Tong Y, Zhao X, Wang R, et al. Therapeutic effect of berberine on chronic atrophic gastritis based on plasma and urine metabolisms. *Eur J Pharmacol*. 2021;908:174335. doi:10.1016/j.ejphar.2021.174335
36. Wang B, Zhou W, Zhang H, et al. Exploring the effect of weifuchun capsule on the toll-like receptor pathway mediated hes6 and immune regulation against chronic atrophic gastritis. *J Ethnopharmacol*. 2023;303:115930. doi:10.1016/j.jep.2022.115930
37. Tong Y, Liu L, Wang R, et al. Berberine attenuates chronic atrophic gastritis induced by mung and its potential mechanism. *Front Pharmacol*. 2021;12:644638. doi:10.3389/fphar.2021.644638
38. Beales IL, Calam J. Interleukin 1 beta and tumour necrosis factor alpha inhibit acid secretion in cultured rabbit parietal cells by multiple pathways. *Gut*. 1998;42(2):227–234. doi:10.1136/gut.42.2.227
39. Unver N, McAllister F. Il-6 family cytokines: key inflammatory mediators as biomarkers and potential therapeutic targets. *Cytokine Growth Factor Rev*. 2018;41:10–17. doi:10.1016/j.cytogfr.2018.04.004
40. Tang X, Chen X, Li X, et al. The tlr4 mediated inflammatory signal pathway might be involved in drug resistance in drug-resistant epileptic rats. *J Neuroimmunol*. 2022;365:577802. doi:10.1016/j.jneuroim.2021.577802
41. Li H, Tang D, Qi C, et al. Forsythiaside inhibits bacterial adhesion on titanium alloy and attenuates ti-induced activation of nuclear factor-kb signaling-mediated macrophage inflammation. *J Orthopaedic Surg Res*. 2018;13(1):139. doi:10.1186/s13018-018-0834-x
42. Zhou X, Zhang L, Lie L, et al. Mxa suppresses tak1-ikka/β-nf-kb mediated inflammatory cytokine production to facilitate mycobacterium tuberculosis infection. *J Infect*. 2020;81(2):231–241. doi:10.1016/j.jinf.2020.05.030
43. Jing C, Sun Z, Xie X, et al. Network pharmacology-based identification of the key mechanism of qinghuo rougan formula acting on uveitis. *Biomed Pharmacother*. 2019;120:109381. doi:10.1016/j.biopha.2019.109381
44. Qiu W, Leibowitz B, Zhang L, et al. Growth factors protect intestinal stem cells from radiation-induced apoptosis by suppressing puma through the pi3k/akt/p53 axis. *Oncogene*. 2010;29(11):1622–1632. doi:10.1038/onc.2009.451
45. Tiemin P, Fanzheng M, Peng X, et al. Muc13 promotes intrahepatic cholangiocarcinoma progression via egfr/pi3k/akt pathways. *J Hepatol*. 2020;72(4):761–773. doi:10.1016/j.jhep.2019.11.021
46. Kim SH, Kim JY, Park SY, et al. Activation of the egfr-pi3k-cam pathway by prl-1-overexpressing placenta-derived mesenchymal stem cells ameliorates liver cirrhosis via er stress-dependent calcium. *Stem Cell Res Ther*. 2021;12(1):551. doi:10.1186/s13287-021-02616-y
47. Jiang R, Tang J, Zhang X, et al. Ccn1 promotes inflammation by inducing il-6 production via alpha6beta1/pi3k/akt/nf-kappa pathway in autoimmune hepatitis. *Front Immunol*. 2022;13:810671. doi:10.3389/fimmu.2022.810671
48. Miao Z, Miao Z, Wang S, et al. Quercetin antagonizes imidacloprid-induced mitochondrial apoptosis through PTEN/PI3K/AKT in grass carp hepatocytes. *Environ Pollut*. 2021;290:118036. doi:10.1016/j.envpol.2021.118036
49. Pappalardo F, Russo G, Candido S, et al. Computational modeling of pi3k/akt and MAPK signaling pathways in melanoma cancer. *PLoS One*. 2016;11(3):e0152104. doi:10.1371/journal.pone.0152104
50. Tsai HF, Hsu PN. Modulation of tumor necrosis factor-related apoptosis-inducing ligand (trail)-mediated apoptosis by helicobacter pylori in immune pathogenesis of gastric mucosal damage. *J Microbiol Immunol Infect*. 2017;50(1):4–9. doi:10.1016/j.jmii.2016.01.002
51. He H, Feng M, Xu H, et al. Total triterpenoids from the fruits of Chaenomeles speciosa exerted gastroprotective activities on indomethacin-induced gastric damage via modulating microRNA-423-5p-mediated tff/nag-1 and apoptotic pathways. *Food Funct*. 2020;11(1):662–679. doi:10.1039/C9FO02322D
52. Han B, Jiang P, Li Z, et al. Coptisine-induced apoptosis in human colon cancer cells (hct-116) is mediated by pi3k/akt and mitochondrial-associated apoptotic pathway. *Phytomedicine*. 2018;48:152–160. doi:10.1016/j.phymed.2017.12.027
53. Wang J, Hu S, Wang J, et al. Fucoidan from acaudina molpadioides protects pancreatic islet against cell apoptosis via inhibition of inflammation in type 2 diabetic mice. *Food Sci Biotechnol*. 2016;25(1):293–300. doi:10.1007/s10068-016-0042-6
54. Wang L, Liu X, Kang Q, et al. Nrf2 overexpression decreases vincristine chemotherapy sensitivity through the pi3k-akt pathway in adult b-cell acute lymphoblastic leukemia. *Front Oncol*. 2022;12:876556. doi:10.3389/fonc.2022.876556
55. Wang J, Wang A, He H, et al. Trametenolic acid b protects against cerebral ischemia and reperfusion injury through modulation of microRNA-10a and pi3k/akt/mtor signaling pathways. *Biomed Pharmacother*. 2019;112:108692. doi:10.1016/j.biopha.2019.108692

56. Zhang Y, Xu H, He H, et al. Total triterpenes from the fruits of *Chaenomeles speciosa* (sweet nakai) protects against indomethacin-induced gastric mucosal injury: involvement of tff1-mediated egf/egfr and apoptotic pathways. *J Pharm Pharmacol*. 2020;72(3):409–423. doi:10.1111/jphp.13207
57. Kim B, Srivastava SK, Kim SH. Caspase-9 as a therapeutic target for treating cancer. *Expert Opin Ther Targets*. 2015;19(1):113–127. doi:10.1517/14728222.2014.961425
58. Meyer AR, Goldenring JR. Injury, repair, inflammation and metaplasia in the stomach. *J Physiol*. 2018;596(17):3861–3867. doi:10.1113/JP275512
59. Ye HY, Shang ZZ, Zhang FY, et al. *Dendrobium huoshanense* stem polysaccharide ameliorates alcohol-induced gastric ulcer in rats through nrf2-mediated strengthening of gastric mucosal barrier. *Int J Biol Macromol*. 2023;236:124001. doi:10.1016/j.ijbiomac.2023.124001
60. Schulzke J, Fromm M. Tight junctions: molecular structure meets function. *Ann NY Acad Sci* 2009;1165(1):1–6. doi:10.1111/j.1749-6632.2009.04925.x
61. Gao A, Xia T, Peng Z, et al. The ethanolic extract of peanut shell attenuates the depressive-like behaviors of mice through modulation of inflammation and gut microbiota. *Food Res Int*. 2023;168:112765. doi:10.1016/j.foodres.2023.112765
62. Ren L, Feng W, Shao J, et al. Diethyldithiocarbamate-copper nanocomplex reinforces disulfiram chemotherapeutic efficacy through light-triggered nuclear targeting. *Theranostics*. 2020;10(14):6384–6398. doi:10.7150/thno.45558
63. Müller SL, Portwich M, Schmidt A, et al. The tight junction protein occludin and the adherens junction protein alpha-catenin share a common interaction mechanism with zo-1. *J Biol Chem*. 2005;280(5):3747–3756. doi:10.1074/jbc.M411365200
64. Derk J, Como C, Jones H, et al. Formation and function of the meningeal arachnoid barrier around the developing mouse brain. *Dev Cell*. 2023;58(8):635–44.e4. doi:10.1016/j.devcel.2023.03.005

Drug Design, Development and Therapy

Dovepress

## Publish your work in this journal

Drug Design, Development and Therapy is an international, peer-reviewed open-access journal that spans the spectrum of drug design and development through to clinical applications. Clinical outcomes, patient safety, and programs for the development and effective, safe, and sustained use of medicines are a feature of the journal, which has also been accepted for indexing on PubMed Central. The manuscript management system is completely online and includes a very quick and fair peer-review system, which is all easy to use. Visit <http://www.dovepress.com/testimonials.php> to read real quotes from published authors.

Submit your manuscript here: <https://www.dovepress.com/drug-design-development-and-therapy-journal>